11-12-2019

A comprehensive resource for induced pluripotent stem cells from patients with primary tauopathies

Celeste M Karch

Rita Martinez

Jacob A Marsh

Simon Hsu

Nupur Ghoshal

See next page for additional authors

Authors

Celeste M Karch, Rita Martinez, Jacob A Marsh, Simon Hsu, Nupur Ghoshal, Joanne Norton, Nigel J Cairns, and et al

Stem Cell Reports
Resource
ISSCR
OPEN ACCESS

A Comprehensive Resource for Induced Pluripotent Stem Cells from Patients with Primary Tauopathies

Celeste M. Karch,[1,*] Aimee W. Kao,[2] Anna Karydas,[2] Khadijah Onanuga,[3] Rita Martinez,[1] Andrea Argouarch,[2] Chao Wang,[4] Cindy Huang,[4] Peter Dongmin Sohn,[4] Kathryn R. Bowles,[5] Salvatore Spina,[2] M. Catarina Silva,[6] Jacob A. Marsh,[1] Simon Hsu,[1] Derian A. Pugh,[5] Nupur Ghoshal,[7] Joanne Norton,[1] Yadong Huang,[4] Suzee E. Lee,[2] William W. Seeley,[2] Panagiotis Theofilas,[8] Lea T. Grinberg,[8] Fermin Moreno,[2] Kathryn McIlroy,[3] Bradley F. Boeve,[9] Nigel J. Cairns,[7] John F. Crary,[5,10] Stephen J. Haggarty,[6] Justin K. Ichida,[11] Kenneth S. Kosik,[12] Bruce L. Miller,[2] Li Gan,[4] Alison M. Goate,[5,13] Sally Temple[3,13,*] Tau Consortium Stem Cell Group

[1]Department of Psychiatry, Washington University in St. Louis School of Medicine, 425 South Euclid Avenue, Campus Box 8134, St. Louis, MO 63110, USA
[2]Division of Memory and Aging Center, Department of Neurology, University of California, San Francisco, San Francisco, CA 94158, USA
[3]Neural Stem Cell Institute, 1 Discovery Drive, Rensselaer, NY 12144, USA
[4]Gladstone Institutes of Neurological Disease, Department of Neurology, Neuroscience Graduate Program, University of California, San Francisco, CA 94158, USA
[5]Ronald M. Loeb Center for Alzheimer's Disease, Departments of Neuroscience, Neurology and Genetics & Genomic Sciences, Icahn School of Medicine, New York, NY 10029, USA
[6]Chemical Neurobiology Laboratory, Center for Genomic Medicine, Departments of Neurology & Psychiatry, Massachusetts General Hospital and Harvard Medical School, Boston, MA 02114, USA
[7]Department of Neurology, Washington University in St. Louis, St. Louis, MO 63110, USA
[8]Department of Pathology and Laboratory Medicine, University of California, San Francisco, San Francisco, CA 94143, USA
[9]Department of Neurology, Mayo Clinic College of Medicine, Rochester, MN, USA
[10]Department of Pathology, Fishberg Department of Neuroscience, Friedman Brain Institute, Icahn School of Medicine at Mount Sinai, New York, NY 10029, USA
[11]Department of Stem Cell Biology and Regenerative Medicine, Keck School of Medicine, University of Southern California, Los Angeles, CA 90033, USA
[12]Department of Molecular Cellular and Developmental Biology, Neuroscience Research Institute, Biomolecular Science and Engineering Program, University of California, Santa Barbara, Santa Barbara, CA, USA
[13]Co-senior author
*Correspondence: karchc@wustl.edu (C.M.K.), sallytemple@neuralsci.org (S.T.)
https://doi.org/10.1016/j.stemcr.2019.09.006

SUMMARY

Primary tauopathies are characterized neuropathologically by inclusions containing abnormal forms of the microtubule-associated protein tau (MAPT) and clinically by diverse neuropsychiatric, cognitive, and motor impairments. Autosomal dominant mutations in the *MAPT* gene cause heterogeneous forms of frontotemporal lobar degeneration with tauopathy (FTLD-Tau). Common and rare variants in the *MAPT* gene increase the risk for sporadic FTLD-Tau, including progressive supranuclear palsy (PSP) and corticobasal degeneration (CBD). We generated a collection of fibroblasts from 140 *MAPT* mutation/risk variant carriers, PSP, CBD, and cognitively normal controls; 31 induced pluripotent stem cell (iPSC) lines from *MAPT* mutation carriers, non-carrier family members, and autopsy-confirmed PSP patients; 33 genome engineered iPSCs that were corrected or mutagenized; and forebrain neural progenitor cells (NPCs). Here, we present a resource of fibroblasts, iPSCs, and NPCs with comprehensive clinical histories that can be accessed by the scientific community for disease modeling and development of novel therapeutics for tauopathies.

INTRODUCTION

Frontotemporal lobar degeneration (FTLD) with inclusions containing the microtubule-associated protein tau (FTLD-Tau) account for half of all cases of FTLD. This heterogeneous group of diseases includes progressive supranuclear palsy (PSP), corticobasal degeneration (CBD), Pick disease, and other rare forms of tauopathy. Patients with FTLD-Tau exhibit a broad range of neurological deficits including movement and motor neuron disease (e.g., gait and balance disturbances, impaired speech and swallowing, visual impairment), psychiatric impairment (e.g., mood and behavior), and cognitive impairment (e.g., memory, executive dysfunction, language and attention) (Perry et al., 2017). Due to significant overlap in the clinical syndromes, a definitive diagnosis can only be obtained by postmortem examination of brain tissue obtained at autopsy or more rarely by biopsy (Perry et al., 2017). Thus, to understand disease etiology, it is particularly valuable to generate a collection of induced pluripotent stem cells (iPSCs) from patients who have been followed clinically and from whom detailed neurological, neuroimaging, and neuropathological data and tissues are available. This requires a coordinated multidisciplinary effort and is the central impetus for the development of the resource described here.

Table 1. Neuropathology in FTLD-Tau Associated with *MAPT* Mutations

Mutation	Clinical	Neuropathology			Tau Isoforms	References[a]	iPSCs Reported
		Macroscopy	Microscopy	Tauopathy			
P301L	bvFTD, personality change, language abnormalities	atrophy of frontal and temporal lobes, basal ganglia, hippocampus, and depigmentation of substantia nigra	neuronal loss, ballooned neurons, and gliosis	neurons: tau-immunoreactive perinuclear, ring-like and dot-like cytoplasmic inclusions, fibrillary neuronal inclusions, and neuropil threads	4R	Mirra et al., 1999	Iovino et al., 2015; Paonessa et al., 2019; Silva et al., 2019
				astrocytes: thorn-shaped inclusions			
				oligodendrocytes: coiled bodies			
S305I	bvFTD, personality change, language abnormalities, Parkinsonism	atrophy of medial temporal lobe, temporal pole, and hippocampus	neuronal loss, gliosis, and ballooned neurons	neurons: tau-immunoreactive fibrillary inclusions and diffuse cytoplasmic staining	4R	Kovacs et al., 2008	N/A
				astrocytes: thorn-shaped inclusions			
				oligodendrocytes: coiled bodies			
				argyrophilic grains			
S305N	bvFTD, personality change, memory loss	atrophy of frontal and temporal lobes	neuronal loss and gliosis	neurons: tau-immunoreactive Pick body-like and ring-like inclusions	4R	Boeve et al., 2005; Iijima et al., 1999	N/A
				astrocytes: thorn-shaped inclusions			
				oligodendrocytes: coiled bodies			
S305S	bvFTD, memory loss	atrophy of frontal and temporal lobes	neuronal loss, gliosis, and ballooned neurons	neurons: tau-immunoreactive neurofibrillary tangles and pretangles	4R	Skoglund et al., 2008; Stanford et al., 2000	N/A
				astrocytes: tuft-shaped inclusions			
				oligodendrocytes: coiled bodies			
IVS10+16	bvFTD, personality change, executive dysfunction, memory loss, parkinsonism, non-fluent aphasia	atrophy of frontal and temporal lobes, cingulate and insular cortex, hippocampus, striatum, amygdala and brainstem	neuronal loss, gliosis, and ballooned neurons	neurons: tau-immunoreactive fibrillary inclusions and diffuse cytoplasmic staining	4R	Janssen et al., 2002; Lantos et al., 2002	Espuny-Camacho et al., 2017; Esteras et al., 2017; Paonessa et al., 2019; Sposito et al., 2015
				astrocytes: thorn-shaped inclusions			
				oligodendrocytes: coiled bodies			

(*Continued on next page*)

Table 1. *Continued*

Mutation	Clinical	Neuropathology			Tau Isoforms	References[a]	iPSCs Reported
		Macroscopy	Microscopy	Tauopathy			
V337M	antisocial behavior, paranoia, executive dysfunction	atrophy of frontal and temporal lobes and hippocampus	neuronal loss and gliosis	neurons: tau-immunoreactive neurofibrillary tangles, pretangles, and neuropil threads astrocytes: tuft-shaped inclusions oligodendrocytes: none	3R & 4R	Spillantini et al., 1996; Spina et al., 2017	Ehrlich et al., 2015; Sohn et al., 2019
G389R	progressive aphasia, apathy, rigidity	atrophy of frontal and temporal lobes, hippocampus, and amygdala	neuronal loss and gliosis	neurons: tau-immunoreactive Pick body-like and filamentous inclusions astrocytes: none oligodendrocytes: none	3R & 4R	Murrell et al., 1999	N/A
R406W	memory loss	severe atrophy of frontal and temporal lobes and hippocampus	neuronal loss, gliosis, and ballooned neurons	neurons: tau-immunoreactive neurofibrillary tangles, Pick body-like inclusions astrocytes: thorn-shaped inclusions oligodendrocytes: coiled bodies	3R & 4R	Miyasaka et al., 2001; Reed et al., 1997	Imamura et al., 2016; Jiang et al., 2018
R406W/ R406W	bvFTD	N/A	N/A	N/A	3R & 4R	Behnam et al., 2015; Ng et al., 2015	N/A

N/A, not available.
[a]See additional references at the AD/FTD Mutation Database (Cruts et al., 2012).

While the majority of patients with primary tauopathy are sporadic, autosomal dominant FTLD-Tau families have been reported to carry mutations in the microtubule-associated protein tau (*MAPT*) gene. More than 50 *MAPT* mutations are reported to cause FTLD-Tau (Table 1; http://www.molgen.ua.ac.be/ADMutations/) (Cruts et al., 2012). The *MAPT* gene is alternatively spliced in the central nervous system (CNS) to produce six tau isoforms that differ based on the presence of the N-terminal insertion (0N, 1N, 2N) and the number of microtubule-binding repeats (MTBR; 3R, 4R; Figure 1). In normal adult human brains, the ratio of 3R/4R tau is 1:1 (Trabzuni et al., 2012). *MAPT* mutation carriers may bear 3-repeat (3R), 4-repeat (4R), or mixed 3R/4R tau inclusions (Table 1) (Cairns et al., 2007).

Several mechanisms have been proposed to explain how *MAPT* mutations cause disease: abnormal *MAPT* splicing, altered microtubule-binding kinetics, impaired degradation, or tau accumulation and aggregation, among others (van Swieten and Spillantini, 2007). We have focused our collection on mutations that represent these proposed mechanisms. A subset of *MAPT* mutations occur at sites that alter *MAPT* splicing, resulting in increased levels of exon 10-containing (4R) mRNA (e.g., IVS10+16, S305I, S305N, S305S) (Liu and Gong, 2008). In the case of intronic mutations such as IVS10+16, no mutant protein is produced. Instead, there is a shift in the levels of 4R tau, skewing the normally balanced 3R/4R tau ratio in human adult brain. Another set of mutations occurs in exon 10, which is exclusively present in 4R tau isoforms (e.g., P301L, P301S) (Hutton et al., 1998). Many of the mutations located in and around exon 10 have been implicated in disrupting microtubule-binding kinetics (Dayanandan et al., 1999; Fischer

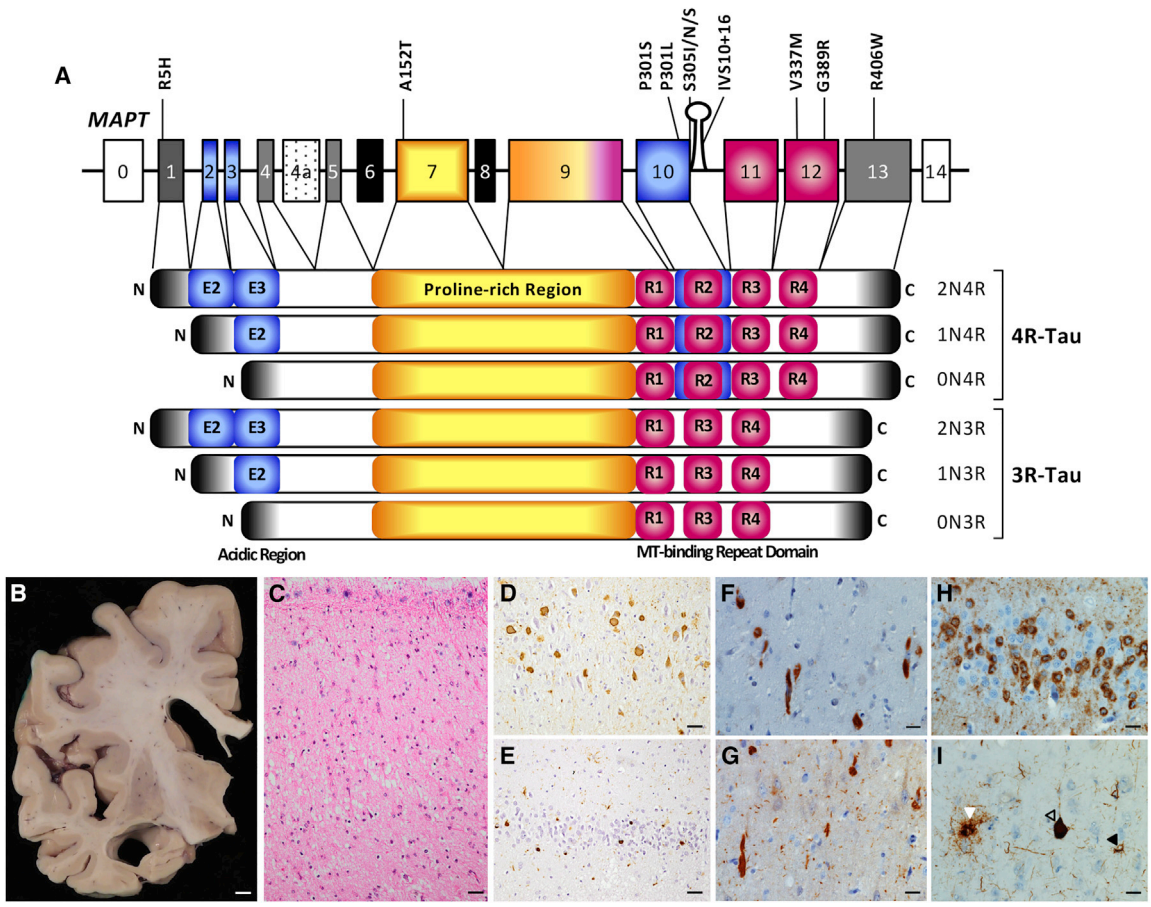

Figure 1. *MAPT* Mutations Cause Primary Tauopathy

(A) Schematic of the location of *MAPT* mutations reported in this collection. *MAPT* A152T, V337M, G389R, and R406W occur in all tau isoforms expressed in the brain. *MAPT* P301L, P301S, and S305I/N/S occur exclusively in transcripts containing exon 10 (2N4R, 1N4R, and 0N4R). *MAPT* P301L/S, S305I/N/S and IVS10+16 alter splicing of tau such that more 4R-containing transcripts are expressed.

(B–I) Neuropathology in human brains with primary tauopathies. (B–E) *MAPT* R406W carrier. (B) Atrophy of the frontal lobe with dilatation of the lateral ventricle and prominent shrinkage of the medial temporal lobe. Scale bar, 0.5 cm. (C) Neuronal loss, gliosis, and microvacuolation of superficial laminae of the superior temporal gyrus. H&E. (D) Neuronal cytoplasmic PHF1-immunoreactive inclusions are seen in the hippocampal CA1 subfield. (E) Pick body-like, PHF1-immunoreactive inclusion bodies in the dentate fascia. Scale bar in (C), (D), and (E), 50 μm. (F and G) Anterior cingulate gyrus of a *MAPT* V337M carrier. (F) RD4-immunoreactive cytoplasmic inclusions in spindle, also called von Economo, neurons and surrounding layer V neurons. (G) R3 (RD3) tau-immunoreactive cytoplasmic inclusions in spindle and surrounding layer V neurons, and in the neuropil. (H) Dentate gyrus of *MAPT* P301L case showing typical pTAU (CP13) ring-like perinuclear deposit and Pick body-like inclusions. (I) PSP associated with a *MAPT* A152T variant. Tufted astrocyte (left; white arrow), neurofibrillary tangle (center; open arrow), and oligodendroglial coiled bodies (right; black arrow), stained with a phospho-tau antibody (CP13). Scale bar, 25 μm.

et al., 2007). Other *MAPT* mutations are located some distance from exon 10 and are expressed by all *MAPT* transcripts (e.g., R5H, V337M, G389R, R406W); thus, their mode of action may be linked to aspects of tau biology beyond microtubule binding, such as membrane association (Gauthier-Kemper et al., 2011). Additionally, all *MAPT* mutations increase the propensity for the tau protein to aggregate. Despite the clear association of *MAPT* mutations with FTLD-Tau, we have little understanding of the mechanisms by which these mutations lead to disease.

Rare and common variants in *MAPT* have been associated with increased risk for PSP, CBD, and frontotemporal dementia (FTD) (Coppola et al., 2012; Höglinger et al., 2011). *MAPT* A152T decreases binding of tau to microtubules and increases tau oligomer formation *in vitro* (Coppola et al., 2012). When expressed in *Caenorhabditis elegans*, *MAPT* A152T induces neuronal dysfunction,

mislocalization of pre-synaptic proteins, and distorted mitochondrial distribution and trafficking, and reduces life span independently of protein aggregation (Butler et al., 2019; Pir et al., 2016). Mouse models expressing A152T demonstrate age-dependent neuronal loss and seizures, which occur both in the presence (Decker et al., 2016) or absence of tau aggregates (Maeda et al., 2016). iPSC-derived neurons from *MAPT* A152T carriers exhibit increased total tau levels and phosphorylation, detergent-insoluble tau, dysregulation of proteostasis pathways involving autophagy and lysosomal activity, and vulnerability to specific cellular stressors (Biswas et al., 2016; Fong et al., 2013; Silva et al., 2016). Our fibroblast and stem cell resource containing *MAPT* variants that are predicted to modify PSP and CBD risk will allow for the cellular and molecular dissection of disease phenotypes.

Patient-derived iPSCs have emerged as a powerful resource to study the molecular mechanisms underlying neurodegenerative diseases. These iPSCs can be differentiated into the neuronal and glial subtypes that are affected in primary tauopathies, giving us a tool toward understanding the biology of tau in a human cell model that may more faithfully reflect the endogenous condition. To date, iPSCs carrying the *MAPT* mutations N279K, P301L, V337M, R406W, and IVS10+16 and the risk variant A152T have been described, and their neural derivatives show phenotypes such as tau accumulation, tau hyperphosphorylation, tau insolubility, vulnerability to specific cellular stressors, and other phenotypes that begin to reveal possible disease mechanisms (Ehrlich et al., 2015; Hallmann et al., 2017; Imamura et al., 2016; Iovino et al., 2015; Jiang et al., 2018; Seo et al., 2017; Silva et al., 2016; Sposito et al., 2015; Wren et al., 2015). Most prior studies, however, have not included genome-edited isogenic controls, which increase the power to detect variant-specific phenotypes by decreasing inter-individual variability. These promising findings warrant the investment in a comprehensive, isogenically controlled collection of *MAPT* iPSC lines.

Here, we present a resource of fibroblast and iPSC lines that includes known disease-associated *MAPT* mutations and paired isogenic iPSCs, *MAPT* risk variant carriers, and PSP-syndrome (PSP-S) and corticobasal syndrome (CBS) lines from individuals where a *MAPT* mutation has not been detected. Most of the cell lines presented in this study were obtained from participants who underwent detailed clinical phenotyping, and for whom fluid biomarkers, imaging biomarkers, and genetic and neuropathological information are available that can be used for correlative analyses with cellular phenotypes. Together, this represents a comprehensive resource that can be accessed for tauopathy modeling and the discovery of novel therapeutics.

RESULTS

Selection of Fibroblast Lines

Dermal fibroblasts were collected from: (1) families with pathogenic *MAPT* mutations; (2) individuals carrying *MAPT* missense variants that increase risk for PSP, CBD, and FTD; (3) sporadic PSP-S and CBS cases; and (4) cognitively normal (non-mutant) controls at the Memory and Aging Center at the University of California San Francisco, the Knight Alzheimer Disease Research Center at Washington University, and the National Institute of Neurological Disease and Stroke (NINDS) Cell Repository. A total of 36 fibroblast lines were generated from individuals with pathogenic *MAPT* mutations (P301L, S305I, IVS10+16, V337M, G389R, R406W; Figure 1 and Table 2). These mutations are representative of some of the most common *MAPT* mutations and capture the range of clinical and neuropathological phenotypes associated with FTLD-Tau (Tables 1 and 2). The collection also includes fibroblasts from eight *MAPT* A152T risk variant carriers, which has been reported to increase the risk for PSP, CBD, and FTD (Coppola et al., 2012). Additionally, we have banked fibroblast lines from research participants clinically diagnosed with PSP-S, CBS, or mixed dementias (Alzheimer's disease and Lewy body disease) and from cognitively normal controls (Table 2). These fibroblasts were obtained from subjects who are part of larger clinical programs that obtain a detailed clinical history, including physical and neurological examinations, cognitive testing, and neuroimaging (magnetic resonance imaging [MRI], β-amyloid positron emission tomography [PET], and tau PET). Many fibroblast lines also have corresponding plasma and cerebrospinal fluid (CSF) samples. Additional covariates for the fibroblast lines including age at biopsy, sex, and genotypic data are available upon request from http://neuralsci.org/tau.

The patient-specific fibroblasts in this collection capture classical aspects of clinical and neuropathology associated with primary tauopathies (Table 1). A *MAPT* R406W carrier presented with progressive memory loss and later developed the behavioral variant of FTD (bvFTD). Macroscopically, there was pronounced atrophy of the temporal lobe (cell line F11362; Figures 1B–1E). Microscopically, there was severe neuronal loss and gliosis and cortical neurofibrillary tangles similar to those seen in Alzheimer's disease. Frequent Pick body-like, tau-immunoreactive inclusions were seen in affected areas including the hippocampus and dentate gyrus. Tau-immunoreactive glial inclusions were also present. A *MAPT* V337M carrier included in the collection exhibited bvFTD; neuropathological examination revealed inclusions containing both 3R and 4R tau (cell line GIH6; Figures 1F and 1G). *MAPT* P301L cases more commonly present clinically with bvFTD, and

Table 2. Dermal Fibroblast Bank to Model Primary Tauopathies

MAPT	Classification	Clinical Presentation	Tau Isoform	Mean AAO[a]	Mean Disease Duration[a]	Fibroblasts	Families
A152T	PSP, CBD, FTLD-Tau	bvFTD	4R	57.5	N/A	8	N/A
P301L	FTLD-Tau	bvFTD	4R	52.6	6.7	13	3
S305I	FTLD-Tau/AGD	bvFTD	4R	39	2	2	1
IVS10+16	FTLD-Tau	bvFTD/AD	4R	49.1	10.3	4	1
V337M	FTLD-Tau	bvFTD	3R & 4R	51.5	15.4	4	2
G389R	FTLD-Tau	bvFTD	3R & 4R	39.8	2.5	3	1
R406W	FTLD-Tau	AD	3R & 4R	56.3	11.5	9	2
R406W/R406W	FTLD-Tau	bvFTD	3R & 4R	34	7	1	1
WT	PSP	PSP-S	4R	N/A	N/A	12	N/A
WT	CBD	CBS	4R	N/A	N/A	5	N/A
WT	PSP/CBD mixed	PSP-S/CBS/mixed	4R	N/A	N/A	10	N/A
WT	normal	N/A	N/A	N/A	N/A	69	N/A

AAO, age at onset; bvFTD, behavioral variant frontotemporal dementia; AGD, argyrophilic grain disease; AD, Alzheimer's disease; PSP, progressive supranuclear palsy; CBD, cortical basal degeneration; N/A, not available.
[a]Data from the AD/FTD Mutation Database presented in years (Cruts et al., 2012).

pathologically display neuronal cytoplasmic inclusions with perinuclear ring-like concentration and the presence of mini Pick body-like inclusions (Figure 1H). A *MAPT* A152T carrier (cell line FTD19; Figure 1I) included in the collection presented with symptoms characteristic of PSP-S, including motor slowing, falls, and cervical dystonia that progressed to dysarthria as well as supranuclear gaze palsy, and neuropathological examination revealed classical PSP neuropathology featuring 4R tau-immunoreactive tufted astrocytes (white arrow in Figure 1I), neurofibrillary tangles (open arrow in Figure 1I), and oligodendroglial coiled bodies (black arrow in Figure 1I).

Generation and Characterization of iPSCs

To establish cellular models that can inform on the pathophysiological mechanisms of *MAPT* mutations, *MAPT* risk variants, and sporadic PSP, including cell types affected by disease, we reprogrammed a subset of fibroblasts described in Table 2 into iPSCs. All iPSCs were generated using non-integrating Sendai virus carrying *SOX2*, *OCT4*, *KLF4*, and *cMYC* (Table 3, Figure 2A). Multiple clones are available for each line. iPSCs were grown in feeder-free conditions using Matrigel and maintained in mTeSR1. Resulting iPSCs have been characterized for pluripotency based on morphology and gene expression markers (Figures 2B and 2C). We confirmed the silencing of exogenous Sendai virus-driven pluripotent markers by qPCR (Figure 2C). Correct mutation propagation was verified by Sanger sequencing (Figure 2D), chromosomal stability was assessed by karyotyping (Figure 2E), and the capacity to form cell types from the three germ layers was also confirmed (Figures 2F and 2G). All iPSC lines reported in this study meet these quality-control criteria (Table S1 and Figure S1), are included in the cell bank, and are available upon request from http://neuralsci.org/tau.

Genome Editing and Characterization of iPSCs

Genetic background of individual donors is a large contributor to phenotypic variability in iPSCs (Kilpinen et al., 2017). To define phenotypes driven specifically by a mutant or risk allele, we used CRISPR/Cas9 genome editing to establish isogenic controls of donor iPSC lines (Figure 2A). For each set of edited lines, additional iPSC clones were selected that underwent the CRISPR/Cas9 editing pipeline but remained unmodified. These unmodified iPSC clones serve as important controls, in addition to the parental donor line, to account for selective pressures that may occur during the editing process (Budde et al., 2017). Donor iPSC lines carrying the *MAPT* mutations IVS10+16, P301L, S305I, R406W, and V337M have been corrected to wild type (WT; Tables 4 and S2).

The most commonly used mouse model of tauopathy overexpresses *MAPT* P301S (Yoshiyama et al., 2007). Clinically, *MAPT* P301S carriers present with a more aggressive form of FTD than *MAPT* P301L carriers and have an earlier age at onset (P301S: mean age at onset 33.7 years and mean disease duration 4.2 years; P301L: mean age at onset 52.6 years and mean disease duration 6.7 years) (Cruts et al.,

Table 3. Human iPSCs for Modeling Primary Tauopathies

Donor ID	Alternative Donor ID	Mutation	Clinical Status[a]	Autopsy	Corrected Line	Fibroblast Source	Neural Induction
FTD30 (FTD-FF)	151209SBA1	A152T/WT	S	pending	no	UCSF	yes
FTD19 (FTD-T)	151209SBA2	A152T/WT	S	PSP	no	UCSF	yes
GIH2	151209SBA3	A152T/WT	A	N/A	no	UCSF	yes
FTD38	151209SBA4	A152T/WT	A	N/A	no	UCSF	yes
GIH169	160311SBA5	A152T/WT	S	N/A	no	UCSF	yes
GIH56	160311SBA6	A152T/WT	S	N/A	no	UCSF	yes
TAU6 (Tau1225-7)	160311SBA7	A152T/WT	S	CBD	no	UCSF	yes
F0510	F0510	P301L/WT	A	N/A	yes	NINDS repository	yes
F13535	F13535	P301L/WT	A	N/A	no	WUSM	N/A
F14537	F14537	P301L/WT	S	FTLD-Tau	no	WUSM	N/A
F14536	F14536	WT/WT[b]	A	N/A	no	WUSM	N/A
MHF110	17524NCE1	S305I/WT	S	N/A	no	UCSF	N/A
75.11	AG255075	S305I/WT	N/A	N/A	yes	ARTFL/LEFFTDS	N/A
300.12	AG251300	S305N/WT	N/A	N/A	no	ARTFL/LEFFTDS	N/A
GP1.1	GP-1i	S305S/WT	N/A	FTLD-Tau	yes	NSWBB	N/A
GIH36	160311SBC1	IVS10+16/WT	A	N/A	yes	UCSF	yes
GIH161	I18XXYYNCG1	WT/WT[b]	A	N/A	no	UCSF	N/A
GIH178	I18XXYYNCC3	IVS10+16/WT	N/A	N/A	no	UCSF	N/A
GIH6	160311SBB1	V337M/WT	S	FTLD-Tau	yes	UCSF	yes
GIH7	160311SBB2	V337M/WT	A	N/A	yes	UCSF	yes
GIH155	160311SBB3	V337M/WT	S	N/A	no	UCSF	N/A
ND32951A	ND32951A	V337M/WT	A	N/A	yes	NINDS repository	yes
MHF100	171018NCD1	G389R/WT	A	N/A	no	UCSF	N/A
MHF101	171018NCD2	G389R/WT	A	N/A	no	UCSF	N/A
MHF102	171018NCD3	G389R/WT	S	N/A	no	UCSF	N/A
F11374	F11374	R406W/WT	A	N/A	no	WUSM	N/A
F11362	F11362	R406W/WT	S	FTLD-Tau	yes	WUSM	yes
F11421	F11421	R406W/WT	A	N/A	yes	WUSM	yes
GIH143	UCSF1	R406W/R406W	S	N/A	no	UCSF	N/A
GIH131	170524NCF1	WT/WT	S	PSP	no	UCSF	N/A
GIH92	171013NCF3	WT/WT	S	PSP	no	UCSF	N/A

UCSF, University of California San Francisco Memory and Aging Center; WUSM, Washington University, Knight Alzheimer's Disease Research Center; NINDS repository, National Institute of Neurologic Disorders and Stroke; ARTFL/LEFFTDS, Advancing Resource and Treatment for Frontotemporal Dementia/Longitudinal Evaluations of Familial Frontotemporal Dementia Subjects; NSWBB, New South Wales Brain Bank; N/A, not available.

[a]At biopsy: A, asymptomatic; S, symptomatic.

[b]Non-carrier, related to MAPT family.

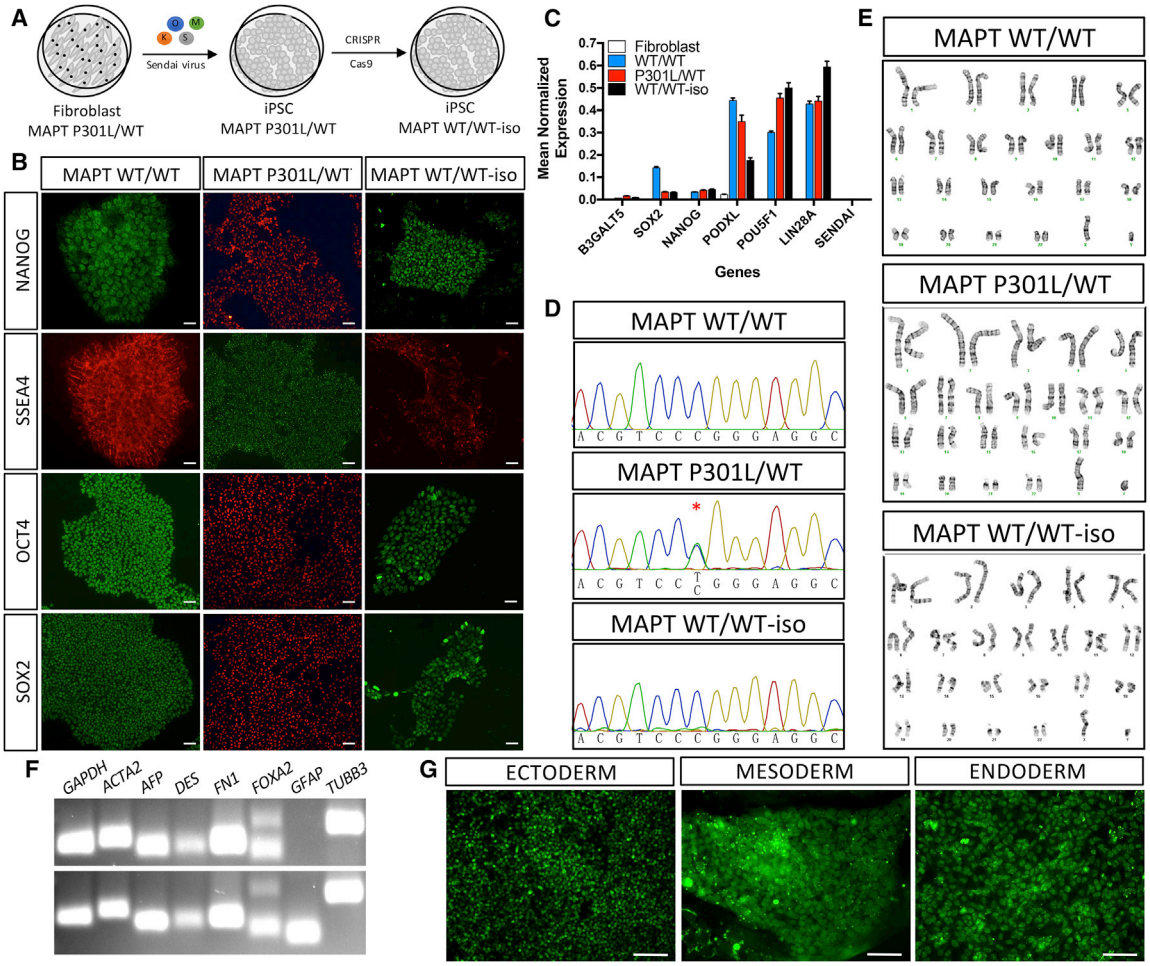

Figure 2. Generation and Characterization of iPSC Models of Tauopathy

Representative images of control (*MAPT* WT/WT), mutant (*MAPT* P301L/WT), and CRISPR/Cas9-edited, isogenic control (*MAPT* WT/WT-iso) iPSCs.

(A) Diagram of reprogramming and CRISPR/Cas9 editing.

(B and C) Immunostaining (B) and qPCR (C) for pluripotency markers. Graph represents mean ± SEM.

(D) Sanger sequencing.

(E) Karyotyping.

(F and G) Spontaneous differentiation into cells within the three germ layers evaluated by RT-PCR (F) and immunostaining (G). *MAPT* WT/WT (iPSC line: F11350); *MAPT* P301L/WT (iPSC line: F0510); *MAPT* WT-iso (iPSC line: F0510.2Δ2′H1). Scale bars, 50 μm.

See also Table S1.

2012). However, fibroblast lines from *MAPT* P301S carriers, which would be useful to validate mouse studies, were not available for reprogramming at the time of this study. Thus, we used CRISPR/Cas9 to mutate the *MAPT* P301L donor iPSC line to *MAPT* P301S (Tables 4 and S2). For this series, we performed whole-genome sequencing and analysis of the mutational burden induced by genome editing and observed no modifications at computationally predicted off-target sites from CRISPR/Cas9 (Budde et al., 2017). The mutational burden that was observed in the edited iPSC lines was largely driven by selective pressures of culture (Bhutani et al., 2016; Budde et al., 2017; Merkle et al., 2017).

To understand the specific contribution of *MAPT* mutations and risk variants to disease phenotypes, we introduced *MAPT* mutations into an unaffected control line. In a control donor iPSC line (F11350) from a male individual carrying *APOE* 3/3 and *MAPT* H1/H1, we introduced *MAPT* R5H, P301L, or G389R (Tables 4 and S2). In a second control iPSC line (F13505) from a female individual carrying *APOE* 3/3 and *MAPT* H1/H1, we introduced *MAPT* S305I or S305S (Tables 4 and S2). All resulting edited or

Table 4. CRISPR/Cas9-Edited iPSC Lines

Donor ID	Donor Genotype	Isogenic Genotype	*Ngn2* Integration	Engineering Method[a]	Line Name	Neural Induction
F11362	R406W/WT	WT/WT	no	CRISPR	F11362.1Δ1C11, F11362.1Δ1B6	yes
F11421	R406W/WT	WT/WT	no	CRISPR	F11421.12Δ2A07	yes
F11374	R406W/WT	N/A	yes	TALENs	NF11374.65	yes
160311SBB1	V337M/WT	WT/WT	no	CRISPR	GIH6C1Δ1E11	yes
160311SBB2	V337M/WT	WT/WT	no	CRISPR	GIH7C2Δ2B12, GIH7C2Δ2F02	yes
ND32951A	V337M/WT	WT/WT	no	CRISPR	ND32951A.15Δ1B06, ND32951A.15Δ1C12	yes
GIH36	IVS10+16/WT	WT/WT	no	CRISPR	GIH36C2Δ1D01	yes
F0510	P301L/WT	WT/WT	no	CRISPR	F0510.2Δ2E7, F0510.2Δ2′H1	yes
F0510	P301L/WT	P301L/P301S	no	CRISPR	F0510.2Δ3A11, F0510.2Δ3A9	yes
F0510	P301L/WT	WT/P301S	no	CRISPR	F0510.2Δ3E10, F0510.2Δ4B3, F0510.2Δ4B4	yes
F0510	P301L/WT	P301S/P301S	no	CRISPR	F0510.2Δ3B5	yes
F0510	P301L/WT	N/A	yes	TALENs	NF0510.23, NF0510.12	yes
75.11	S305I/WT	WT/WT	no	CRISPR	75.11-IW1A12	N/A
75.11	S305I/WT	S305I/S305I	no	CRISPR	75.11-IH1B9	N/A
GP1.1	S305S/WT	S305S/S305S	no	CRISPR	GP1.1-SH1G8	N/A
F13505	WT/WT	S305I/WT	no	CRISPR	F13505.1-I1B10	N/A
F13505	WT/WT	S305S/WT	no	CRISPR	F13505.1-S3H5	N/A
F11350	WT/WT	WT/R5H	no	CRISPR	F11350.1.R5HΔ2F06	N/A
F11350	WT/WT	WT/G389R	no	CRISPR	F11350.1.G389R.1C05ΔE03	N/A
F11350	WT/WT	P301L/P301L	no	CRISPR	F11350.1.P301LΔ4A02, F11350.1.P301LΔ4A08	N/A
F12468	WT/WT	N/A	yes	TALENs	NF12468.131	yes
WTC11	WT/WT	N/A	yes	TALENs	NWTC11.G3	yes
WTC11	WT/WT	WT/WT	yes	TALENs/CRISPR	NWTC11.G3.0036	yes
WTC11	WT/WT	V337M/WT	yes	TALENs/CRISPR	NWTC11.G3.0212	yes
WTC11	WT/WT	V337M/V337M	yes	TALENs/CRISPR	NWTC11.G3.3917	yes

[a]*Ngn2* was engineered by TALENs; *MAPT* mutations/corrections were engineered by CRISPR/Cas9.

unmodified clones were characterized for pluripotency and chromosomal stability as described above (Table S2). We are continuing to build this collection on the same genetic background with additional *MAPT* mutations.

Differentiation of iPSCs into Neural Progenitor Cells and Differentiated Neural Cells

iPSCs have the capacity to form the diverse neural cell types affected by primary tauopathies. By exploiting our understanding of CNS development, several groups have established protocols to generate neuroectodermal neural progenitor cells (NPCs) that can be further patterned into specific neuronal subtypes (Doi et al., 2014; Elkabetz et al., 2008; Muratore et al., 2014). We adapted a neural aggregate-based method that allows for the efficient generation of a scalable pool of NPCs, which have the capacity to be patterned into cultures enriched for different types of neurons or glia (Figure 3). Production of cryopreserved

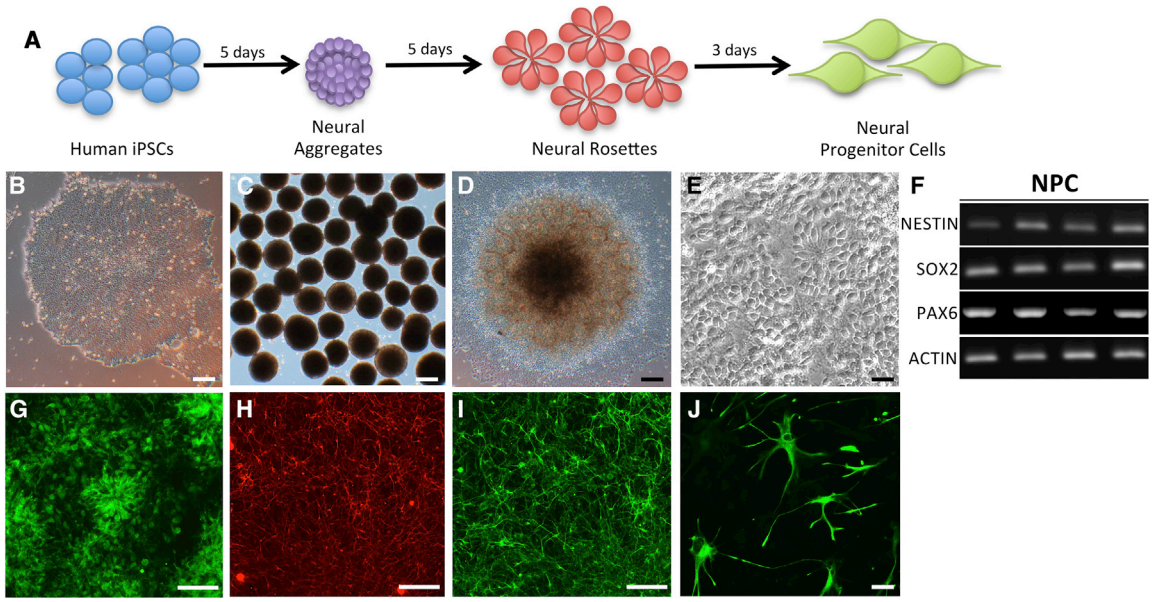

Figure 3. Differentiation of iPSCs into Neural Progenitor Cells

(A) Diagram for neural progenitor derivation protocol.

(B–E) Bright-field images. (B) iPSC. (C) Neural aggregates. (D) Neural rosettes. (E) NPCs.

(F) RT-PCR of neural progenitor cell markers, *NESTIN*, *SOX2*, *PAX6*, and the housekeeping gene, *ACTIN*.

(G) Immunostaining for neural progenitor cell marker, PAX6.

(H and I) Immunostaining of iPSC-derived neurons. (H) Tuj1. (I) MAP2.

(J) Immunostaining of iPSC-derived astrocytes with GFAP.

Scale bars, 50 μm.

banks of stable and expandable intermediate NPC populations will help to reduce time, effort, and variability across experiments.

We have applied this neural induction protocol to the donor lines in this collection across multiple laboratories (Figure S1; Tables S1 and S2). We have verified that the iPSC collection presented here has the capacity to form NPCs that can be expanded and cryopreserved (Figures 3A–3E). These NPCs express early neuroectodermal markers including PAX6, SOX2, and Nestin, and lack expression of SOX10, which marks the neural crest, indicating a CNS expression pattern (Figure 3F). The viability of these NPCs after thaw is high (mean 89% ± 1.2% live cells). These NPCs maintain their capacity to differentiate into neuronal subtypes when used at early passages (between passage 1 and passage 5), while astrocyte differentiation as measured by glial fibrillary acidic protein (GFAP) and S100β can be promoted using NPCs from early or later passages (beyond passage 5). By incorporating fluorescence-activated cell sorting for cell-surface markers $CD133^{+}$, $CD184^{+}$, and $CD271^{-}$, the resulting selected pool of NPCs can be maintained with a high proportion of neuronal differentiation for at least 50 passages (Cheng et al., 2017). It is critical to culture NPCs at a high density for the successful maintenance of a stable and expandable population of progenitors (Cheng et al., 2017).

NPCs can be patterned into different neural CNS regions and differentiated into neuronal and glial subtypes to model primary tauopathies (Figures 3I and 3J) (Jiang et al., 2018; Silva et al., 2016; Tcw et al., 2017). By default, these NPCs tend to adopt anterior CNS characteristics, such as *FOXG1* expression, but this fate can also be stimulated by the addition of patterning factors (Kirwan et al., 2015; Saurat et al., 2016). The resulting forebrain neurons produce tau that is physiologically similar to human CNS tau (Sato et al., 2018), with the exception of intracellular 4R tau levels. Achieving splicing of the six major tau isoforms expressed in adult brains remains a challenge in the iPSC system (Hefti et al., 2018; Sposito et al., 2015). Despite the low levels of 4R tau, iPSC-derived neural cells from *MAPT* mutation/risk variant carriers phenocopy aspects of primary tauopathies. This includes the accumulation of phosphorylated forms of tau (Ehrlich et al., 2015; Imamura et al., 2016; Iovino et al., 2015; Silva et al., 2016, 2019), mitochondrial defects (Esteras et al., 2017), and increased cell vulnerability (Hallmann et al., 2017; Silva et al., 2016; Wren et al., 2015). More recently, we have demonstrated that neurons expressing *MAPT*

R406W (F11362) capture molecular signatures related to altered synaptic function that are also present in human brains from *MAPT* R406W carriers and in mouse models of primary tauopathies (Jiang et al., 2018). Cryopreserved NPCs from the iPSCs reported here (Tables 3 and 4) are available upon request from http://neuralsci.org/tau.

Generation of Integrated, Isogenic, and Inducible Neurogenin-2 iPSCs

Integrated, isogenic, and inducible neurogenin-2 (i^3N) iPSCs engineered with a doxycycline-inducible mouse Neurogenin-2 (*Ngn2*) transgene in the AAVS1 safe-harbor locus can be scalably differentiated to homogeneous excitatory neurons, which enables the use of human neurons for high-throughput drug discovery (Wang et al., 2017). We have engineered two healthy control WT (F12468 and WTC11), as well as *MAPT* P301L (F0510) and *MAPT* R406W (F11374), to i^3N iPSCs (Table 4) (Wang et al., 2017). We also mutagenized a control i^3N line (WTC11) to be heterozygous or homozygous for *MAPT* V337M (Sohn et al., 2019). All modified lines were characterized for chromosomal stability, and confirmed for *Ngn2* integration and neuronal differentiation (Figure S2 and Table S2), and are available upon request from http://neuralsci.org/tau.

DISCUSSION

We present a comprehensive and valuable resource that can be used to model primary tauopathies and for drug discovery. Our patient-based cohort consists of a library of 140 dermal fibroblast lines and respective iPSC lines with multiple clones that are focused on primary tauopathies: 29 iPSC lines from patients carrying pathogenic *MAPT* mutations or risk variants; 2 iPSC lines from autopsy-confirmed PSP patients; 28 isogenic iPSCs; and 8 *Ngn2*-integrated iPSCs. Importantly, most of these cell lines were obtained from deeply clinically phenotyped individuals with detailed neurological and neuropsychological assessment and availability of fluid biomarkers (CSF and plasma), imaging biomarkers (MRI, β-amyloid PET, and tau PET), genetic data, and, for some, neuropathological data.

Phenotypic Diversity of MAPT Mutations

More than 50 mutations in *MAPT* have been reported to cause FTLD-Tau and are located primarily in exons 9–13; yet FTLD-Tau is both clinically and neuropathologically heterogeneous (Table 1). Broadly, FTLD-Tau is defined by neuronal loss, gliosis, and spongiform changes in layer II with predominant involvement of the frontal, temporal, cingulate, and insular cortices and variable involvement of subcortical nuclei. Clinically, patients with FTLD-Tau pathology can present with a broad range of phenotypes spanning behavioral, cognitive, and motor disturbances. Various different combinations of clinical symptoms may be seen in association with specific mutations and even among affected members of a single family (Spina et al., 2008). Hence, there is a need to understand the impact of specific *MAPT* mutations within the genetic background of individuals with known clinical and pathological manifestations. Our fibroblast and iPSC resources allow for the investigation of common and unique cellular phenotypes driven by these mutations.

The Clinical and Pathological Spectrum of the Most Common 4R Primary Tauopathies

FTLD-Tau, PSP, and CBD are neuropathologically defined as 4R tauopathies (Kovacs, 2015). PSP pathology occurs in neurons and glia (astrocytes and oligodendrocytes) and preferentially affects the tectum, tegmentum, globus pallidus, diencephalon, and superior cerebellar peduncle (Dickson et al., 2007). In CBD, neuronal and glial pathology occurs within gray and white mater regions of the cortex, basal ganglia, diencephalon, and rostral brainstem (Forman et al., 2002). While 4R-tau aggregation is characteristic of both PSP and CBD, differences in proteolytic processing of tau have been reported to distinguish the two diseases: detergent-insoluble tau occurs at a doublet around 37 kDa in CBD and as a single band at 33 kDa in PSP (Arai et al., 2001, 2004). The *MAPT* A152T risk variant has been associated with both clinical and pathological forms of PSP-S/PSP and CBS/CBD. Our fibroblast resources containing sporadic PSP-S and CBS will allow for the cellular and molecular dissection of disease phenotypes, providing a powerful system for understanding the cellular mechanisms that drive phenotypic differences between PSP-S/PSP and CBS/CBD.

Challenges in Modeling Primary Tauopathies in Traditional Cell and Mouse Models

Current cellular and animal models used to study primary tauopathies have several limitations. Critically, there is no natural animal model of tauopathy, as these diseases are largely restricted to *Homo sapiens* (Heuer et al., 2012; Holzer et al., 2004). While tau isoforms may share broad functional similarities, different isoforms likely play distinct physiological and pathological roles in the cell (Goedert and Jakes, 1990; Karch et al., 2012; Kosik et al., 1989; Panda et al., 2003). Notably, the expression of tau isoforms drastically differs between human and rodent brains. While the adult human brains have roughly equal levels of 3R and 4R tau, adult rodents express almost exclusively 4R tau, limiting the conclusions that can be drawn from mouse models (Trabzuni et al., 2012). Additionally, most cellular

and transgenic models (e.g., *C. elegans*, *Drosophila*, and mice) rely on overexpression of a mutant transgene comprising a single tau isoform, which may produce effects that are a function of excessive protein expression, specific isoform expression, and possible off-target effects, rather than a disease-relevant phenotype. Finally, neuronal and glial cells are the primary cell types affected in tauopathies; therefore, studies in immortalized cell lines may fail to capture the phenotypes specific to neurons and glia. Thus, our understanding of how tau is metabolized in the human brain has been obtained from experimental paradigms that do not fully capture physiological conditions relevant to human tauopathies. Stem cell models begin to address these gaps; however, tau generated by stem cell-derived neurons remains in the fetal state (e.g., primarily 3R0N) (Hefti et al., 2018; Iovino et al., 2015; Sposito et al., 2015). Nevertheless, cells expressing 4R-containing *MAPT* mutations, such as P301L, exhibit altered tau phosphorylation, tau accumulation, and cell vulnerability (Iovino et al., 2015; Silva et al., 2019). These phenotypes can be reversed with novel tau degraders (Silva et al., 2019).

Basic Science, Clinical, and Translational Applications of Human Tauopathy Models

Beyond modeling the molecular and cellular pathophysiology of primary tauopathies, the derivation of patient-specific expandable NPCs enables large-scale functional genomics, proteomics, and small-molecule-based and CRISPR-based genetic modifier screens (Boselli et al., 2017; Cheng et al., 2017; Silva et al., 2016; Tian et al., 2019; Wang et al., 2017). This includes the use of high-content imaging methodologies with subcellular level resolution of molecular and morphological changes in defined neuronal subtypes with and without glial subtypes. We envision that using the framework of phenotypes from the autosomal dominant mutations and risk factors for tauopathy described here will also assist in the interpretation of genetic variants of unknown pathological significance that are being identified by exome and whole-genome sequencing projects.

One of the challenges in modeling diseases that typically present clinically in mid to late adulthood is to accelerate aging in iPSC-derived cells. This is particularly difficult given that during reprogramming to pluripotency, the features of aging present in originating somatic cells are reset. In contrast, fibroblasts directly reprogrammed into neurons retain their aging characteristics such as DNA methylation (Huh et al., 2016; Maherali et al., 2007; Mertens et al., 2015). Efforts to induce chronological aging in iPSC-derived neurons are under way (Miller et al., 2013). In the meantime, the ability to study both reprogrammed iPSCs and their source fibroblasts directly differentiated into neurons may help the field dissect how gene mutations contribute to the neurodegenerative process at both early and late age-dependent stages.

Our intention is to extend the existing resource, particularly by adding fibroblasts and iPSCs carrying novel mutations with clear pathogenicity and unique clinical features such as those associated with extremely early age of onset or rapid disease progression. Other variants in specific domains of tau or in non-coding genomic elements (e.g., 5′/3′ UTRs, enhancer sites) would also be of interest to the collection as well as additional genome engineering in existing lines.

Conclusions

In total, the resource presented here represents an opportunity to understand the mechanisms by which pathogenic mutations or risk variants in *MAPT* drive tauopathy. This resource will also be of interest to the broader community working on neurodegenerative disease. The collaborative efforts through which this resource has been generated can serve as a model for other neurodegenerative disease subtypes as well as other neurological and non-neurological diseases under genetic influence. Our intention is to broadly share the collection of fibroblasts, iPSCs, and NPCs and related data and information, which are available upon request. We are continuing to build this collection with additional reprogramming and genome editing, and updates will be available at http://neuralsci.org/tau (Figure S3).

EXPERIMENTAL PROCEDURES

The Washington University and University of California San Francisco Institutional Review Boards reviewed the Neuropathology Cores (from whom the brains were obtained) operating protocols as well as this specific study and determined it was exempt from approval. Our participants provide this consent by signing the hospital's autopsy form. If the participant does not provide future consent before death the DPOA or next of kin provide it after death. All data were analyzed anonymously.

Skin punches were performed following written informed consent from the donor. The informed consent was approved by the Washington University School of Medicine and the University of California San Francisco Institutional Review Board and Ethics Committee (IRB 201104178, 201306108 and 10-03946). The consent allows for use of tissue by all parties, commercial and academic, for the purposes of research but not for use in human therapy.

Peripheral blood mononuclear cells or dermal fibroblasts were transduced with non-integrating Sendai virus carrying OCT3/4, SOX2, KLF4, and cMYC. iPSC lines were analyzed for pluripotency markers by immunocytochemistry (ICC) and qPCR; spontaneous differentiation into the three germ layers by ICC or qPCR; and chromosomal abnormalities by karyotyping. Human iPSCs were edited using CRISPR/Cas9 as previously reported (Budde et al.,

2017). i^{3}N iPSCs were generated as described previously (Wang et al., 2017). See Supplemental Experimental Procedures for additional details.

SUPPLEMENTAL INFORMATION

Supplemental Information can be found online at https://doi.org/10.1016/j.stemcr.2019.09.006.

CONSORTIA

Tau Consortium Stem Cell Group: Carolina Alquezar[1], Kathryn R. Bowles[2], David C. Butler[3], John F. Crary[4], Li Gan[5], Alison M. Goate[2], Stephen J. Haggarty[6], Israel Hernandez[7], Valerie Hennes[8], Cindy Huang[5], Justin K. Ichida[8], Martin Kampmann[9], Aimee W. Kao[1], Celeste M. Karch[10], Anna Karydas[1], Kenneth S. Kosik[7], Rita Martinez[10], Khadijah Onanuga[3], M. Catarina Silva[6], Sally Temple[3], Chao Wang[5]

[1]Division of Memory and Aging Center, Department of Neurology, University of California, San Francisco, San Francisco, CA 94158, USA

[2]Ronald M. Loeb Center for Alzheimer's Disease, Departments of Neuroscience, Neurology and Genetics & Genomic Sciences, Icahn School of Medicine, New York, NY 10029, USA

[3]Neural Stem Cell Institute, 1 Discovery Drive, Rensselaer, NY 12144, USA

[4]Department of Pathology, Fishberg Department of Neuroscience, Friedman Brain Institute, Ronald M. Loeb Center for Alzheimer's Disease, Icahn School of Medicine at Mount Sinai, New York, NY 10029, USA

[5]Gladstone Institutes of Neurological Disease, Department of Neurology, Neuroscience Graduate Program, University of California, San Francisco, CA 94158

[6]Chemical Neurobiology Laboratory, Center for Genomic Medicine, Departments of Neurology & Psychiatry, Massachusetts General Hospital and Harvard Medical School, Boston, MA 02114, USA

[7]Department of Molecular Cellular and Developmental Biology, Neuroscience Research Institute, Biomolecular Science and Engineering Program, University of California, Santa Barbara, Santa Barbara, CA, USA

[8]Department of Stem Cell Biology and Regenerative Medicine, Keck School of Medicine, University of Southern California, Los Angeles, CA 90033, USA

[9]Department of Biochemistry and Biophysics, Institute for Neurodegenerative Diseases and California Institute for Quantitative Biomedical Research, University of California, San Francisco, CA 94158, USA

[10]Department of Psychiatry, Washington University in St. Louis, St. Louis, MO 63110, USA

AUTHOR CONTRIBUTIONS

Conceived and designed experiments: C.M.K., A.W.K., C.W., M.C.S., S.J.H., J.K.I., K.S.K., L.G., A.M.G., and S.T. Performed experiments: C.M.K., R.M., J.A.M., A.A., K.R.B., D.A.P., P.T., S.S., S.H., C.W., C.H., P.D.S., D.B., M.C.S., and N.J.C. Analyzed data: C.M.K., A.W.K., A.K., K.M., A.A., S.H., C.W., C.H., and P.D.S. Contributed reagents, materials, and analysis tools: C.M.K., A.W.K., A.K., K.R.B., K.M., Y.H., S.E.L., N.G., J.N., F.M., B.F.B., M.C.S., S.J.H., J.F.C., J.K.I., B.L.M., L.G., L.T.G., W.W.S., A.M.G., K.O., and S.T. Wrote the manuscript: C.M.K., A.W.K., S.S., and S.T. Edited the manuscript: C.M.K., C.W., L.T.G., M.C.S., S.J.H., J.K.I., K.S.K., L.G., A.M.G., S.T., N.G., M.K., N.J.C., and J.F.C.

ACKNOWLEDGMENTS

We would like to thank the research subjects and their families who generously participated in this study. We thank Steven Lotz, Shawn Sutton, Brian Unruh, Isabel Tian, and Nicholas St. John at NeuraCell and Evan Y. Snyder and Yang M. Lui at Sanford Burnham Prebys Medical Discovery Institute for technical assistance. We thank the Icahn School of Medicine at Mount Sinai Pluripotent Stem Cell Core facility for technical assistance. The gRNAs were generated by the Genome Engineering and iPSC Center (GEiC) at the Washington University in St. Louis. We thank Amber Neilson at the GEiC for technical assistance. This work was supported by access to equipment made possible by the Hope Center for Neurological Disorders, and the Departments of Neurology and Psychiatry at Washington University School of Medicine. Data collection and dissemination of the data presented in this paper were supported by the LEFFTDS & ARTFL Consortium (LEFFTDS: U01AG045390; ARTFL: U54NS092089). The authors acknowledge the invaluable contributions of the participants in ARTFL & LEFFTDS as well as the assistance of the support staff at each of the participating sites. Funding: The Tau Consortium (C.M.K., A.W.K., Y.H., S.E.L., J.F.C., S.J.H., J.K.I., K.S.K., B.L.M., L.G., A.M.G., S.T., K.O., M.K.), NIH AG046374 (C.M.K.), CurePSP (A.W.K., K.R.B.), Brain Research Foundation (A.W.K.), MGH Research Scholars Program (S.J.H.), Association for Frontotemporal Degeneration, AFTD (M.C.S., K.R.B.), BrightFocus Foundation (K.R.B.), Farrell Family Alzheimer's Disease Research Fund (C.M.K.), NIH/NIA (P50 AG023501, P01 AG019724, T32 AG023481-11S1, and P50 AG1657303 to B.L.M.), NIH (R01AG054008 and R01NS095252 to J.F.C.), NIH (P50 AG005681 to J.C.M.), NIH (K12 HD001459 to N.G.), NIH/NINDS (R35 NS097277 to S.T.), NIH/NIA (AG056293 to S.T.), NIH (K08 AG052648 to S.S.), NIH (U01 AG045390 to B.B.), NIH U54 NS092089, U24 AG21886. Neuracell received support from the Empire State Stem Cell Fund through New York State Department of Health contract #C029158. Opinions expressed here are solely those of the authors and do not necessarily reflect those of the Empire State Stem Cell Board, the New York State Department of Health, or the State of New York. J.K.I. is a New York Stem Cell Foundation-Robertson Investigator. A.W.K. and M.K. are Paul G. Allen Family Foundation Distinguished Investigators. M.K. is a Chan Zuckerberg Biohub Investigator. A.M.G. is a member of the Scientific Advisory Board for Denali Therapeutics and on the Genetic Scientific Advisory Panel for Pfizer. N.J.C. is a member of the Modeling Alliance of Systems Pharmacology in Tauopathies Scientific Advisory Board. S.J.H. is a member of the Scientific Advisory Board for Rodin Therapeutics, Frequency Therapeutics, and Psy Therapeutics and Souvien Therapeutics, none of whom had involvement in the present study. N.G. has participated or is currently participating in clinical trials of anti-dementia drugs sponsored by Bristol Myers Squibb, Eli Lilly/Avid Radiopharmaceuticals, Janssen Immunotherapy, Novartis, Pfizer, Wyeth, SNIFF (The Study of Nasal Insulin to Fight Forgetfulness) study, and A4 (The Anti-Amyloid Treatment in Asymptomatic Alzheimer's

Disease) trial. S.T. is president of StemCultures, scientific co-founder of Luxa Biotech and has served on the scientific advisory boards of Sana Biotechnology and Blue Rock Therapeutics and as consultant to Merck. The remaining authors declare no competing interests.

Received: April 5, 2018
Revised: September 16, 2019
Accepted: September 17, 2019
Published: October 17, 2019

REFERENCES

Arai, T., Ikeda, K., Akiyama, H., Nonaka, T., Hasegawa, M., Ishiguro, K., Iritani, S., Tsuchiya, K., Iseki, E., Yagishita, S., et al. (2004). Identification of amino-terminally cleaved tau fragments that distinguish progressive supranuclear palsy from corticobasal degeneration. Ann. Neurol. *55*, 72–79.

Arai, T., Ikeda, K., Akiyama, H., Tsuchiya, K., Yagishita, S., and Takamatsu, J. (2001). Intracellular processing of aggregated tau differs between corticobasal degeneration and progressive supranuclear palsy. Neuroreport *12*, 935–938.

Behnam, M., Ghorbani, F., Shin, J.H., Kim, D.S., Jang, H., Nouri, N., Sedghi, M., Salehi, M., Ansari, B., and Basiri, K. (2015). Homozygous MAPT R406W mutation causing FTDP phenotype: a unique instance of a unique mutation. Gene *570*, 150–152.

Bhutani, K., Nazor, K.L., Williams, R., Tran, H., Dai, H., Dzakula, Z., Cho, E.H., Pang, A.W., Rao, M., Cao, H., et al. (2016). Whole-genome mutational burden analysis of three pluripotency induction methods. Nat. Commun. *7*, 10536.

Biswas, M.H.U., Almeida, S., Lopez-Gonzalez, R., Mao, W., Zhang, Z., Karydas, A., Geschwind, M.D., Biernat, J., Mandelkow, E.M., Futai, K., et al. (2016). MMP-9 and MMP-2 contribute to neuronal cell death in iPSC models of frontotemporal dementia with MAPT mutations. Stem Cell Reports *7*, 316–324.

Boeve, B.F., Tremont-Lukats, I.W., Waclawik, A.J., Murrell, J.R., Hermann, B., Jack, C.R., Jr., Shiung, M.M., Smith, G.E., Nair, A.R., Lindor, N., et al. (2005). Longitudinal characterization of two siblings with frontotemporal dementia and parkinsonism linked to chromosome 17 associated with the S305N tau mutation. Brain *128*, 752–772.

Boselli, M., Lee, B.H., Robert, J., Prado, M.A., Min, S.W., Cheng, C., Silva, M.C., Seong, C., Elsasser, S., Hatle, K.M., et al. (2017). An inhibitor of the proteasomal deubiquitinating enzyme USP14 induces tau elimination in cultured neurons. J. Biol. Chem. *292*, 19209–19225.

Budde, J., Martinez, R., Hsu, S., Wen, N., Chen, J., Coppola, G., Goate, A.M., Cruchaga, C., and Karch, C.M. (2017). Precision genome-editing with CRISPR/Cas9 in human induced pluripotent stem cells. bioRxiv https://doi.org/10.1101/187377.

Butler, V.J., Salazar, D.A., Soriano-Castell, D., Alves-Ferreira, M., Dennissen, F.J.A., Vohra, M., Oses-Prieto, J.A., Li, K.H., Wang, A.L., Jing, B., et al. (2019). Tau/MAPT disease-associated variant A152T alters tau function and toxicity via impaired retrograde axonal transport. Hum. Mol. Genet. *28*, 1498–1514.

Cairns, N.J., Bigio, E.H., Mackenzie, I.R.A., Neumann, M., Lee, V.M.-Y., Hatanpaa, K.J., White, C.L., Schneider, J.A., Grinberg, L.T., Halliday, G., et al. (2007). Neuropathologic diagnostic and nosologic criteria for frontotemporal lobar degeneration: consensus of the Consortium for Frontotemporal Lobar Degeneration. Acta Neuropathol. *114*, 5–22.

Cheng, C., Fass, D.M., Folz-Donahue, K., MacDonald, M.E., and Haggarty, S.J. (2017). Highly expandable human iPS cell-derived neural progenitor cells (NPC) and neurons for central nervous system disease modeling and high-throughput screening. Curr. Protoc. Hum. Genet. *92*, 21 28 21.

Coppola, G., Chinnathambi, S., Lee, J.J., Dombroski, B.A., Baker, M.C., Soto-Ortolaza, A.I., Lee, S.E., Klein, E., Huang, A.Y., Sears, R., et al. (2012). Evidence for a role of the rare p.A152T variant in MAPT in increasing the risk for FTD-spectrum and Alzheimer's diseases. Hum. Mol. Genet. *21*, 3500–3512.

Cruts, M., Theuns, J., and Van Broeckhoven, C. (2012). Locus-specific mutation databases for neurodegenerative brain diseases. Hum. Mutat. *33*, 1340–1344.

Dayanandan, R., Van Slegtenhorst, M., Mack, T.G., Ko, L., Yen, S.H., Leroy, K., Brion, J.P., Anderton, B.H., Hutton, M., and Lovestone, S. (1999). Mutations in tau reduce its microtubule binding properties in intact cells and affect its phosphorylation. FEBS Lett. *446*, 228–232.

Decker, J.M., Kruger, L., Sydow, A., Dennissen, F.J., Siskova, Z., Mandelkow, E., and Mandelkow, E.M. (2016). The Tau/A152T mutation, a risk factor for frontotemporal-spectrum disorders, leads to NR2B receptor-mediated excitotoxicity. EMBO Rep. *17*, 552–569.

Dickson, D.W., Rademakers, R., and Hutton, M.L. (2007). Progressive supranuclear palsy: pathology and genetics. Brain Pathol. *17*, 74–82.

Doi, D., Samata, B., Katsukawa, M., Kikuchi, T., Morizane, A., Ono, Y., Sekiguchi, K., Nakagawa, M., Parmar, M., and Takahashi, J. (2014). Isolation of human induced pluripotent stem cell-derived dopaminergic progenitors by cell sorting for successful transplantation. Stem Cell Reports *2*, 337–350.

Ehrlich, M., Hallmann, A.L., Reinhardt, P., Arauzo-Bravo, M.J., Korr, S., Ropke, A., Psathaki, O.E., Ehling, P., Meuth, S.G., Oblak, A.L., et al. (2015). Distinct neurodegenerative changes in an induced pluripotent stem cell model of frontotemporal dementia linked to mutant TAU protein. Stem Cell Reports *5*, 83–96.

Elkabetz, Y., Panagiotakos, G., Al Shamy, G., Socci, N.D., Tabar, V., and Studer, L. (2008). Human ES cell-derived neural rosettes reveal a functionally distinct early neural stem cell stage. Genes Dev. *22*, 152–165.

Espuny-Camacho, I., Arranz, A.M., Fiers, M., Snellinx, A., Ando, K., Munck, S., Bonnefont, J., Lambot, L., Corthout, N., Omodho, L., et al. (2017). Hallmarks of Alzheimer's disease in stem-cell-derived human neurons transplanted into mouse brain. Neuron *93*, 1066–1081.e8.

Esteras, N., Rohrer, J.D., Hardy, J., Wray, S., and Abramov, A.Y. (2017). Mitochondrial hyperpolarization in iPSC-derived neurons from patients of FTDP-17 with 10+16 MAPT mutation

leads to oxidative stress and neurodegeneration. Redox. Biol. *12*, 410–422.

Fischer, D., Mukrasch, M.D., Von Bergen, M., Klos-Witkowska, A., Biernat, J., Griesinger, C., Mandelkow, E., and Zweckstetter, M. (2007). Structural and microtubule binding properties of tau mutants of frontotemporal dementias. Biochemistry *46*, 2574–2582.

Fong, H., Wang, C., Knoferle, J., Walker, D., Balestra, M.E., Tong, L.M., Leung, L., Ring, K.L., Seeley, W.W., Karydas, A., et al. (2013). Genetic correction of tauopathy phenotypes in neurons derived from human induced pluripotent stem cells. Stem Cell Reports *1*, 226–234.

Forman, M.S., Zhukareva, V., Bergeron, C., Chin, S.S., Grossman, M., Clark, C., Lee, V.M., and Trojanowski, J.Q. (2002). Signature tau neuropathology in gray and white matter of corticobasal degeneration. Am. J. Pathol. *160*, 2045–2053.

Gauthier-Kemper, A., Weissmann, C., Golovyashkina, N., Sebo-Lemke, Z., Drewes, G., Gerke, V., Heinisch, J.J., and Brandt, R. (2011). The frontotemporal dementia mutation R406W blocks tau's interaction with the membrane in an annexin A2-dependent manner. J. Cell Biol *192*, 647–661.

Goedert, M., and Jakes, R. (1990). Expression of separate isoforms of human tau protein: correlation with the tau pattern in brain and effects on tubulin polymerization. EMBO J. *9*, 4225–4230.

Hallmann, A.L., Arauzo-Bravo, M.J., Mavrommatis, L., Ehrlich, M., Ropke, A., Brockhaus, J., Missler, M., Sterneckert, J., Scholer, H.R., Kuhlmann, T., et al. (2017). Astrocyte pathology in a human neural stem cell model of frontotemporal dementia caused by mutant TAU protein. Sci. Rep. *7*, 42991.

Hefti, M.M., Farrell, K., Kim, S., Bowles, K.R., Fowkes, M.E., Raj, T., and Crary, J.F. (2018). High-resolution temporal and regional mapping of MAPT expression and splicing in human brain development. PLoS One *13*, e0195771.

Heuer, E., Rosen, R.F., Cintron, A., and Walker, L.C. (2012). Nonhuman primate models of Alzheimer-like cerebral proteopathy. Curr. Pharm. Des. *18*, 1159–1169.

Höglinger, G.U., Melhem, N.M., Dickson, D.W., Sleiman, P.M.A., Wang, L.-S., Klei, L., Rademakers, R., de Silva, R., Litvan, I., Riley, D.E., et al. (2011). Identification of common variants influencing risk of the tauopathy progressive supranuclear palsy. Nat. Genet. *43*, 699–705.

Holzer, M., Craxton, M., Jakes, R., Arendt, T., and Goedert, M. (2004). Tau gene (MAPT) sequence variation among primates. Gene *341*, 313–322.

Huh, C.J., Zhang, B., Victor, M.B., Dahiya, S., Batista, L.F., Horvath, S., and Yoo, A.S. (2016). Maintenance of age in human neurons generated by microRNA-based neuronal conversion of fibroblasts. eLife *5*. https://doi.org/10.7554/eLife.18648.

Hutton, M., Lendon, C.L., Rizzu, P., Baker, M., Froelich, S., Houlden, H., Pickering-Brown, S., Chakraverty, S., Isaacs, A., Grover, A., et al. (1998). Association of missense and 5'-splice-site mutations in tau with the inherited dementia FTDP-17. Nature *393*, 702–705.

Iijima, M., Tabira, T., Poorkaj, P., Schellenberg, G.D., Trojanowski, J.Q., Lee, V.M., Schmidt, M.L., Takahashi, K., Nabika, T., Matsumoto, T., et al. (1999). A distinct familial presenile dementia with a novel missense mutation in the tau gene. Neuroreport *10*, 497–501.

Imamura, K., Sahara, N., Kanaan, N.M., Tsukita, K., Kondo, T., Kutoku, Y., Ohsawa, Y., Sunada, Y., Kawakami, K., Hotta, A., et al. (2016). Calcium dysregulation contributes to neurodegeneration in FTLD patient iPSC-derived neurons. Sci. Rep. *6*, 34904.

Iovino, M., Agathou, S., Gonzalez-Rueda, A., Del Castillo Velasco-Herrera, M., Borroni, B., Alberici, A., Lynch, T., O'Dowd, S., Geti, I., Gaffney, D., et al. (2015). Early maturation and distinct tau pathology in induced pluripotent stem cell-derived neurons from patients with MAPT mutations. Brain *138*, 3345–3359.

Janssen, J.C., Warrington, E.K., Morris, H.R., Lantos, P., Brown, J., Revesz, T., Wood, N., Khan, M.N., Cipolotti, L., Fox, N.C., et al. (2002). Clinical features of frontotemporal dementia due to the intronic tau 10(+16) mutation. Neurology *58*, 1161–1168.

Jiang, S., Wen, N., Li, Z., Dube, U., Del Aguila, J., Budde, J., Martinez, R., Hsu, S., Fernandez, M.V., Cairns, N.J., et al. (2018). Integrative system biology analyses of CRISPR-edited iPSC-derived neurons and human brains reveal deficiencies of presynaptic signaling in FTLD and PSP. Transl. Psychiatry *8*, 265.

Karch, C.M., Jeng, A.T., and Goate, A.M. (2012). Extracellular tau levels are influenced by variability in tau that is associated with tauopathies. J. Biol. Chem. *287*, 42751–42762.

Kilpinen, H., Goncalves, A., Leha, A., Afzal, V., Alasoo, K., Ashford, S., Bala, S., Bensaddek, D., Casale, F.P., Culley, O.J., et al. (2017). Common genetic variation drives molecular heterogeneity in human iPSCs. Nature *546*, 370–375.

Kirwan, P., Turner-Bridger, B., Peter, M., Momoh, A., Arambepola, D., Robinson, H.P., and Livesey, F.J. (2015). Development and function of human cerebral cortex neural networks from pluripotent stem cells in vitro. Development *142*, 3178–3187.

Kosik, K.S., Orecchio, L.D., Bakalis, S., and Neve, R.L. (1989). Developmentally regulated expression of specific tau sequences. Neuron *2*, 1389–1397.

Kovacs, G.G. (2015). Invited review: neuropathology of tauopathies: principles and practice. Neuropathol. Appl. Neurobiol. *41*, 3–23.

Kovacs, G.G., Pittman, A., Revesz, T., Luk, C., Lees, A., Kiss, E., Tariska, P., Laszlo, L., Molnar, K., Molnar, M.J., et al. (2008). MAPT S305I mutation: implications for argyrophilic grain disease. Acta Neuropathol. *116*, 103–118.

Lantos, P.L., Cairns, N.J., Khan, M.N., King, A., Revesz, T., Janssen, J.C., Morris, H., and Rossor, M.N. (2002). Neuropathologic variation in frontotemporal dementia due to the intronic tau 10(+16) mutation. Neurology *58*, 1169–1175.

Liu, F., and Gong, C.-X. (2008). Tau exon 10 alternative splicing and tauopathies. Mol. Neurodegener. *3*, 8.

Maeda, S., Djukic, B., Taneja, P., Yu, G.Q., Lo, I., Davis, A., Craft, R., Guo, W., Wang, X., Kim, D., et al. (2016). Expression of A152T human tau causes age-dependent neuronal dysfunction and loss in transgenic mice. EMBO Rep. *17*, 530–551.

Maherali, N., Sridharan, R., Xie, W., Utikal, J., Eminli, S., Arnold, K., Stadtfeld, M., Yachechko, R., Tchieu, J., Jaenisch, R., et al. (2007).

Directly reprogrammed fibroblasts show global epigenetic remodeling and widespread tissue contribution. Cell Stem Cell *1*, 55–70.

Merkle, F.T., Ghosh, S., Kamitaki, N., Mitchell, J., Avior, Y., Mello, C., Kashin, S., Mekhoubad, S., Ilic, D., Charlton, M., et al. (2017). Human pluripotent stem cells recurrently acquire and expand dominant negative P53 mutations. Nature *545*, 229–233.

Mertens, J., Paquola, A.C.M., Ku, M., Hatch, E., Bohnke, L., Ladjevardi, S., McGrath, S., Campbell, B., Lee, H., Herdy, J.R., et al. (2015). Directly reprogrammed human neurons retain aging-associated transcriptomic signatures and reveal age-related nucleocytoplasmic defects. Cell Stem Cell *17*, 705–718.

Miller, J.D., Ganat, Y.M., Kishinevsky, S., Bowman, R.L., Liu, B., Tu, E.Y., Mandal, P.K., Vera, E., Shim, J.W., Kriks, S., et al. (2013). Human iPSC-based modeling of late-onset disease via progerin-induced aging. Cell Stem Cell *13*, 691–705.

Mirra, S.S., Murrell, J.R., Gearing, M., Spillantini, M.G., Goedert, M., Crowther, R.A., Levey, A.I., Jones, R., Green, J., Shoffner, J.M., et al. (1999). Tau pathology in a family with dementia and a P301L mutation in tau. J. Neuropathol. Exp. Neurol. *58*, 335–345.

Miyasaka, T., Morishima-Kawashima, M., Ravid, R., Heutink, P., van Swieten, J.C., Nagashima, K., and Ihara, Y. (2001). Molecular analysis of mutant and wild-type tau deposited in the brain affected by the FTDP-17 R406W mutation. Am. J. Pathol. *158*, 373–379.

Muratore, C.R., Srikanth, P., Callahan, D.G., and Young-Pearse, T.L. (2014). Comparison and optimization of hiPSC forebrain cortical differentiation protocols. PLoS One *9*, e105807.

Murrell, J.R., Spillantini, M.G., Zolo, P., Guazzelli, M., Smith, M.J., Hasegawa, M., Redi, F., Crowther, R.A., Pietrini, P., Ghetti, B., et al. (1999). Tau gene mutation G389R causes a tauopathy with abundant pick body-like inclusions and axonal deposits. J. Neuropathol. Exp. Neurol. *58*, 1207–1226.

Ng, A.S., Sias, A.C., Pressman, P.S., Fong, J.C., Karydas, A.M., Zanto, T.P., De May, M., Coppola, G., Geschwind, D.H., Miller, B.L., et al. (2015). Young-onset frontotemporal dementia in a homozygous tau R406W mutation carrier. Ann. Clin. Transl Neurol. *2*, 1124–1128.

Panda, D., Samuel, J.C., Massie, M., Feinstein, S.C., and Wilson, L. (2003). Differential regulation of microtubule dynamics by three- and four-repeat tau: implications for the onset of neurodegenerative disease. Proc. Natl. Acad. Sci. U S A *100*, 9548–9553.

Paonessa, F., Evans, L.D., Solanki, R., Larrieu, D., Wray, S., Hardy, J., Jackson, S.P., and Livesey, F.J. (2019). microtubules deform the nuclear membrane and disrupt nucleocytoplasmic transport in tau-mediated frontotemporal dementia. Cell Rep. *26*, 582–593.e5.

Perry, D.C., Brown, J.A., Possin, K.L., Datta, S., Trujillo, A., Radke, A., Karydas, A., Kornak, J., Sias, A.C., Rabinovici, G.D., et al. (2017). Clinicopathological correlations in behavioural variant frontotemporal dementia. Brain *140*, 3329–3345.

Pir, G.J., Choudhary, B., Mandelkow, E., and Mandelkow, E.M. (2016). Tau mutant A152T, a risk factor for FTD/PSP, induces neuronal dysfunction and reduced lifespan independently of aggregation in a C. elegans Tauopathy model. Mol. Neurodegener. *11*, 33.

Reed, L.A., Grabowski, T.J., Schmidt, M.L., Morris, J.C., Goate, A., Solodkin, A., Van Hoesen, G.W., Schelper, R.L., Talbot, C.J., Wragg, M.A., et al. (1997). Autosomal dominant dementia with widespread neurofibrillary tangles. Ann. Neurol. *42*, 564–572.

Sato, C., Barthelemy, N.R., Mawuenyega, K.G., Patterson, B.W., Gordon, B.A., Jockel-Balsarotti, J., Sullivan, M., Crisp, M.J., Kasten, T., Kirmess, K.M., et al. (2018). Tau kinetics in neurons and the human central nervous system. Neuron *97*, 1284–1298.e7.

Saurat, N.G., Livesey, F.J., and Moore, S. (2016). Cortical differentiation of human pluripotent cells for in vitro modeling of Alzheimer's disease. Methods Mol. Biol. *1303*, 267–278.

Seo, J., Kritskiy, O., Watson, L.A., Barker, S.J., Dey, D., Raja, W.K., Lin, Y.T., Ko, T., Cho, S., Penney, J., et al. (2017). Inhibition of p25/Cdk5 attenuates tauopathy in mouse and iPSC models of frontotemporal dementia. J. Neurosci. *37*, 9917–9924.

Silva, M.C., Cheng, C., Mair, W., Almeida, S., Fong, H., Biswas, M.H.U., Zhang, Z., Huang, Y., Temple, S., Coppola, G., et al. (2016). Human iPSC-derived neuronal model of tau-A152T frontotemporal dementia reveals tau-mediated mechanisms of neuronal vulnerability. Stem Cell Reports *7*, 325–340.

Silva, M.C., Ferguson, F.M., Cai, Q., Donovan, K.A., Nandi, G., Patnaik, D., Zhang, T., Huang, H.T., Lucente, D.E., Dickerson, B.C., et al. (2019). Targeted degradation of aberrant tau in frontotemporal dementia patient-derived neuronal cell models. eLife *8*. https://doi.org/10.7554/eLife.45457.

Skoglund, L., Viitanen, M., Kalimo, H., Lannfelt, L., Jonhagen, M.E., Ingelsson, M., Glaser, A., and Herva, R. (2008). The tau S305S mutation causes frontotemporal dementia with parkinsonism. Eur. J. Neurol. *15*, 156–161.

Sohn, P., Tracy, T., Huang, C., Yan, R., Camargo, C., Mok, S., Freilich, R., Roberson, E., Karch, C., Gestwicki, J., et al. (2019). Pathogenic Tau impairs axon initial segment plasticity and excitability homeostasis. Neuron https://doi.org/10.1016/j.neuron.2019.08.008.

Spillantini, M.G., Crowther, R.A., and Goedert, M. (1996). Comparison of the neurofibrillary pathology in Alzheimer's disease and familial presenile dementia with tangles. Acta Neuropathol. *92*, 42–48.

Spina, S., Farlow, M.R., Unverzagt, F.W., Kareken, D.A., Murrell, J.R., Fraser, G., Epperson, F., Crowther, R.A., Spillantini, M.G., Goedert, M., et al. (2008). The tauopathy associated with mutation +3 in intron 10 of Tau: characterization of the MSTD family. Brain *131*, 72–89.

Spina, S., Schonhaut, D.R., Boeve, B.F., Seeley, W.W., Ossenkoppele, R., O'Neil, J.P., Lazaris, A., Rosen, H.J., Boxer, A.L., Perry, D.C., et al. (2017). Frontotemporal dementia with the V337M MAPT mutation: tau-PET and pathology correlations. Neurology *88*, 758–766.

Sposito, T., Preza, E., Mahoney, C.J., Seto-Salvia, N., Ryan, N.S., Morris, H.R., Arber, C., Devine, M.J., Houlden, H., Warner, T.T., et al. (2015). Developmental regulation of tau splicing is disrupted in stem cell-derived neurons from frontotemporal dementia patients with the 10 + 16 splice-site mutation in MAPT. Hum. Mol. Genet. *24*, 5260–5269.

Stanford, P.M., Halliday, G.M., Brooks, W.S., Kwok, J.B., Storey, C.E., Creasey, H., Morris, J.G., Fulham, M.J., and Schofield, P.R. (2000). Progressive supranuclear palsy pathology caused by a novel silent mutation in exon 10 of the tau gene: expansion of the disease phenotype caused by tau gene mutations. Brain *123* (Pt 5), 880–893.

Tcw, J., Wang, M., Pimenova, A.A., Bowles, K.R., Hartley, B.J., Lacin, E., Machlovi, S.I., Abdelaal, R., Karch, C.M., Phatnani, H., et al. (2017). An efficient platform for astrocyte differentiation from human induced pluripotent stem cells. Stem Cell Reports *9*, 600–614.

Tian, R., Gachechiladze, M.A., Ludwig, C.H., Laurie, M.T., Hong, J.Y., Nathaniel, D., Prabhu, A.V., Fernandopulle, M.S., Patel, R., Abshari, M., et al. (2019). CRISPR interference-based platform for multimodal genetic screens in human iPSC-derived neurons. Neuron https://doi.org/10.1016/j.neuron.2019.07.014.

Trabzuni, D., Wray, S., Vandrovcova, J., Ramasamy, A., Walker, R., Smith, C., Luk, C., Gibbs, J.R., Dillman, A., Hernandez, D.G., et al. (2012). MAPT expression and splicing is differentially regulated by brain region: relation to genotype and implication for tauopathies. Hum. Mol. Genet. *21*, 4094–4103.

van Swieten, J., and Spillantini, M.G. (2007). Hereditary frontotemporal dementia caused by Tau gene mutations. Brain Pathol. *17*, 63–73.

Wang, C., Ward, M.E., Chen, R., Liu, K., Tracy, T.E., Chen, X., Xie, M., Sohn, P.D., Ludwig, C., Meyer-Franke, A., et al. (2017). Scalable production of iPSC-derived human neurons to identify Tau-lowering compounds by high-content screening. Stem Cell Reports *9*, 1221–1233.

Wren, M.C., Zhao, J., Liu, C.C., Murray, M.E., Atagi, Y., Davis, M.D., Fu, Y., Okano, H.J., Ogaki, K., Strongosky, A.J., et al. (2015). Frontotemporal dementia-associated N279K tau mutant disrupts subcellular vesicle trafficking and induces cellular stress in iPSC-derived neural stem cells. Mol. Neurodegener. *10*, 46.

Yoshiyama, Y., Higuchi, M., Zhang, B., Huang, S.-M., Iwata, N., Saido, T.C., Maeda, J., Suhara, T., Trojanowski, J.Q., and Lee, V.M.-Y. (2007). Synapse loss and microglial activation precede tangles in a P301S tauopathy mouse model. Neuron *53*, 337–351.

Stem Cell Reports, Volume *13*

Supplemental Information

A Comprehensive Resource for Induced Pluripotent Stem Cells from Patients with Primary Tauopathies

Celeste M. Karch, Aimee W. Kao, Anna Karydas, Khadijah Onanuga, Rita Martinez, Andrea Argouarch, Chao Wang, Cindy Huang, Peter Dongmin Sohn, Kathryn R. Bowles, Salvatore Spina, M. Catarina Silva, Jacob A. Marsh, Simon Hsu, Derian A. Pugh, Nupur Ghoshal, Joanne Norton, Yadong Huang, Suzee E. Lee, William W. Seeley, Panagiotis Theofilas, Lea T. Grinberg, Fermin Moreno, Kathryn McIlroy, Bradley F. Boeve, Nigel J. Cairns, John F. Crary, Stephen J. Haggarty, Justin K. Ichida, Kenneth S. Kosik, Bruce L. Miller, Li Gan, Alison M. Goate, Sally Temple, and Tau Consortium Stem Cell Group

Supplemental Information

Supplemental Figures

Supplemental Tables

Supplemental Experimental Procedures

Supplemental References, related to Supplemental Experimental Procedures

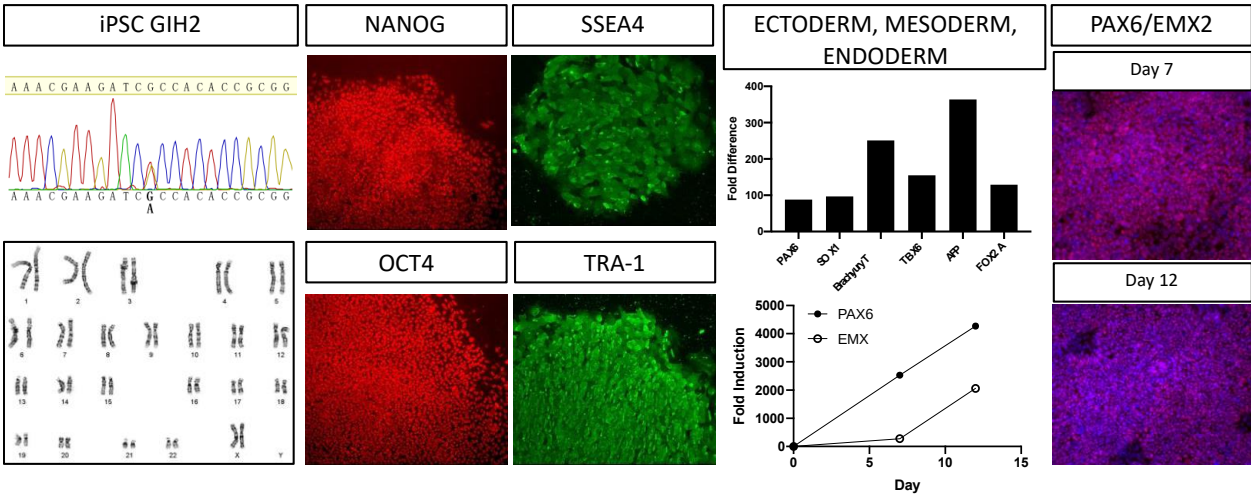

Figure S1: Characterization of iPSC Lines, Related to Table 3. Representative characterization for iPSC lines reported in Table 3 including Sanger sequencing; karyotyping; immunostaining for pluripotency markers; qPCR for gene markers of endoderm, mesoderm, and ectoderm; and neural induction measured by qPCR and immunostaining for PAX6 and EMX2. All available clones have passed QC. Cell line shown, GIH2. See also Table S1.

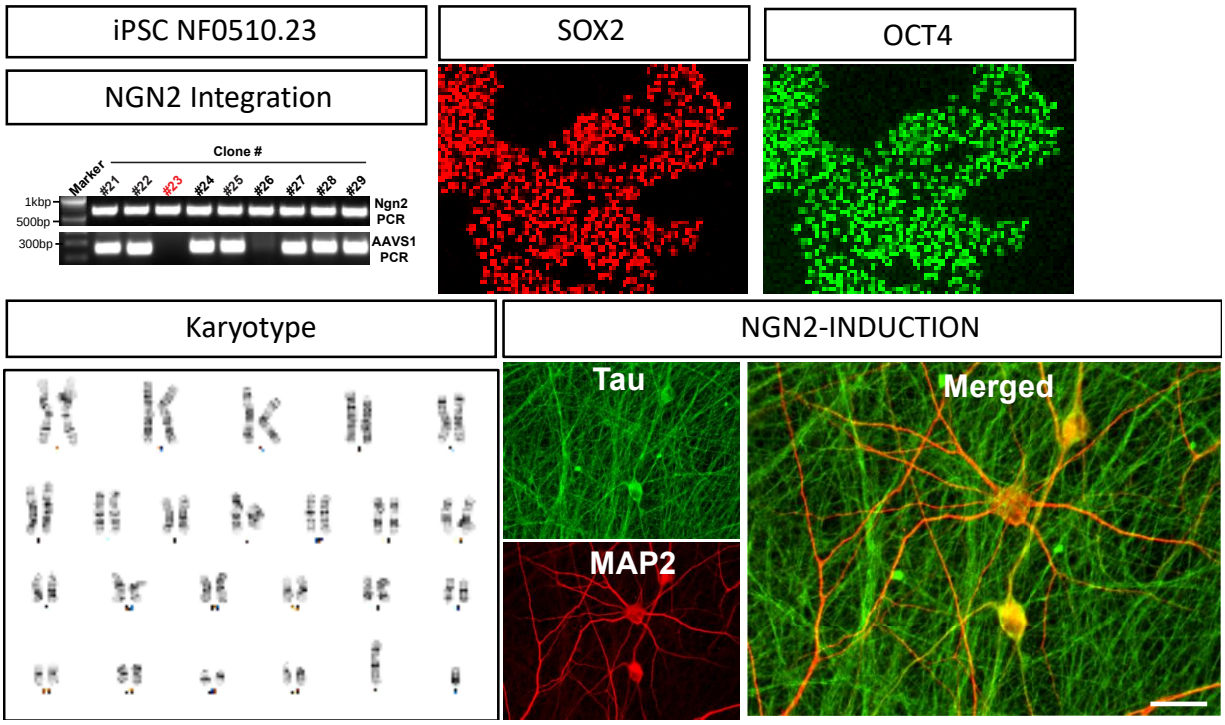

Figure S2: Characterization of Genome-Edited iPSC Lines, Related to Table 4. Representative characterization for cell lines reported in Table 4 including *Ngn2* integration; immunostaining for pluripotency markers; karyotyping; Ngn2-induction reveals cells that are Tau and MAP2 positive. All available lines have by passed QC. Cell line shown, NF0510.23.

SHIP DATE: _____

Lab: _____

Please find enclosed:

# of Vials	Line Name	Gender	Ethnicity	Clinical Phenotype	MAPT Mutation	APOE Genotype	MAPT Haplotype	Fully Characterized	iPSC Reprogramming Method

Figure S3: Representative datasheet for iPSC lines, Related to Tables 3 and 4.

Supplemental Experimental Procedures

Patient Consent

The Washington University and University of California San Francisco Institutional Review Boards reviewed the Neuropathology Cores (from whom the brains were obtained) operating protocols as well as this specific study and determined it was exempt from approval. Our participants provide this consent by signing the hospital's autopsy form. If the participant does not provide future consent before death the DPOA or next of kin provide it after death. All data were analyzed anonymously.

Skin punches were performed following written informed consent from the donor. The informed consent was approved by the Washington University School of Medicine and the University of California San Francisco Institutional Review Board and Ethics Committee (IRB 201104178, 201306108 and 10-03946). The consent allows for use of tissue by all parties, commercial and academic, for the purposes of research but not for use in human therapy.

Neuropathology

The brain of the *MAPT* R406W carrier was evaluated at Washington University. The brains of the *MAPT* A152T, P301L, and V337M carriers were evaluated at University of California San Francisco. Immunohistochemistry against phosphorylated tau was performed with PHF1 and CP13 antibodies (generous gift of Peter Davies). 3R and 4R tau immunohistochemistry was performed with RD4 (Millipore 05-804) and RD3 (Millipore 05-803) antibodies. FTLD-Tau neuropathology was assessed as previously described (Murray et al., 2014; Perry et al., 2017).

Dermal Fibroblast Isolation

To isolate dermal fibroblasts, the epidermal biopsies (3mm skin punch obtained from the proximal thigh or buttock) were rinsed with PBS and cut lengthwise with dissecting scissors. The resulting tissue sections were then plated into a dry 24-well tissue culture-treated plate (approximately 6-12 sections) or 3-4 sections into a 6-well plate, for a total of 18-24 sections per sample. After removing excess PBS from the wells, fibroblast growth media (Lonza, Cat. No. CC-3132) was carefully added, a coverslip was lightly overlaid, and tissue was incubated at 37°C and 5% CO_2. After 24 hours, tissue was supplemented with 1mL fibroblast growth medium and medium changes were repeated every 3-4 days. Fibroblast cells were observed to migrate from the tissue within 2 weeks of culture. Dermal fibroblasts were maintained in fibroblast growth media supplemented with penicillin/streptomycin. Prior to cryopreservation, fibroblasts were tested for Mycoplasma (Lonza). Fibroblasts were cryopreserved at $2x10^5$ cells/vial in equal volumes fibroblast growth media and 2x freezing media (FBS supplemented with 20% DMSO).

iPSC Generation and Characterization

To reprogram cells from *MAPT* S305I and *MAPT* S305N mutation carriers, peripheral blood mononuclear cells (PBMC) were cultured to expand the erythroblast population. PBMCs or dermal fibroblasts were transduced with non-integrating Sendai virus carrying OCT3/4, SOX2, KLF4, and cMYC (Life Technologies) (Ban et al., 2011; Takahashi and Yamanaka, 2006). Cells that showed morphological evidence of reprogramming were selected manually. IPSC lines were characterized using standard methods (Takahashi and Yamanaka, 2006). Each line was analyzed for pluripotency markers by immunocytochemistry (ICC) and quantitative PCR (qPCR); for spontaneous differentiation into the three germ layers by ICC and qPCR; and for chromosomal abnormalities by karyotyping (see below for details). Mutation status was confirmed in newly generated iPSC by Sanger sequencing.

iPSC Culture, Banking and Routine Quality Control Measures

Human iPSC were cultured in mTesR1 on Matrigel-coated tissue culture-treated plates; StembeadsFGF2 (StemCultures, LLC) were used as needed to reduce feeding frequency. For routine passaging and unless otherwise noted below, iPSCs were dissociated with Accutase for 3 minutes. Dissociated cells were collected in PBS and centrifuged at 750 rpm for 3 minutes. After medium was aspirated, a portion of the cells were plated on new Matrigel-coated plates in mTesR1. iPSCs were maintained with less than 5% spontaneous differentiation. Karyotyping and Sanger sequencing, to verify mutation status, was performed every 20 passages.

Genome Editing of iPSC

Human iPSCs were edited using CRISPR/Cas9 as previously reported (Budde et al., 2017). Briefly, allele-specific guideRNAs (gRNAs) were designed for the target allele. gRNAs were designed to have at least 3bp of mismatch to any other gene in the human genome and validated for activity using the T7E1 assay. In this assay, the

T7E1 enzyme recognizes and cleaves non-perfectly matched DNA. To prepare cells for editing, iPSC colonies were dissociated into single cells via incubation in Accutase for 10 minutes. Single cell iPSC cultures were maintained on Matrigel supplemented with fibronectin and cultured in mTesR. To edit cells, human iPSCs were nucleofected with 1μg pMaxGFP (used to assess nucleofection efficiency), 1μg gRNA, 3μg Cas9, and 300μM single stranded oligodeoxynucleotides (ssODN) and the P3 Primary Cell 4D reaction mix (Lonza). To edit *MAPT* S305I and *MAPT* S305N mutant lines and control line F13505.1, human iPSCs were maintained on Matrigel and cultured in StemFlex (Life Technologies). For each edit, $2x10^6$ cells were electroporated using the Neon transfection system (Life Tecnologies) with 4ug gRNA expressing Cas9 vector, and 40μM ssODN. At least 96 clones were screened for editing. We routinely selected 2-5 edited clones for expansion and characterization. In addition to edited clones, we selected 1-2 unedited clones that were exposed to the genome-editing pipeline but remained unmodified. Characterization of edited and unedited clones included qPCR and ICC for pluripotency markers, karyotyping and Sanger sequencing of on and predicted off-target sites.

i^3N iPSCs were generated as described previously (Wang et al., 2017). Briefly, donor vector (pUCM-*Ngn2*) containing AAVS1 homology arm, Tet-ON 3G controlled *Ngn2* transgene and splicing acceptor-linked puromycin was integrated to AAVS1 locus of human iPSCs using a TALEN nuclease pair targeting the AAVS1 locus. Human iPSCs were transfected with donor vector and TALEN pair using DNA-In Stem transfection reagent (MTI-GlobalStem), followed by a puromycin clonal selection. Six clones from each human iPSC line were selected for expansion and characterization. Characterization included PCR reactions for *Ngn2* integration, karyotyping and two-step neuronal differentiation (Sohn et al., 2019; Wang et al., 2017).

iPSC Differentiation into Neural Progenitor Cells

IPSCs were harvested for neural aggregate formation upon reaching 75-85% confluency. IPSCs were dissociated with Accutase (MP Biomedicals) and pelleted by centrifugation. Cells were counted and resuspended in mTesR1 supplemented with the ROCK inhibitor Y-27632 (10μM) to achieve 450-650,000 cells/mL. Then, 100μL/well of iPSC suspension was plated into a v-bottom 96-well plate. The v-bottom plate was centrifuged at 750 rpm for 3 minutes to pellet the iPSCs and promote formation of spheres. Cells were then incubated at 37°C, 5% CO_2 for 24 hrs. Neurospheres were cultured for 5 additional days with daily media change in Neural Induction Medium (NIM; Stemcell Technologies).

On Day 5 of neural aggregate formation, spheres were washed with 100μL of DMEM/F12. Then, 100μL of NIM was added to each well. Spheres were transferred from the conical wells into a 6-well plate, pre-coated with poly-Ornithin (PLO)/Laminin (Millpore-Sigma), at a density of 32 spheres per well. Daily media changes followed with NIM. Spheres were monitored daily for formation of neural rosette structures. Neural rosettes were harvested when spheres had completely flattened and clusters were clearly visible (3-7 days after plating; line dependent). Neural rosettes were harvested by aspirating spent medium, washing with DMEM/F12, and then adding 1mL of Neural Rosette Selection reagent (Stemcell Technologies) to each well for 1hr at 37°C. Rosette clusters were then detached by pipetting with DMEM/F12. Rosette clusters were transferred into a conical tube, centrifuged at 750 rpm for 3 minutes, and then either cryopreserved or plated for neural progenitor cell expansion.

To cryopreserve cells, equal volumes of NIM and 2x neural freezing medium (20% DMSO in Knockout Serum Replacement Medium, ThermoFisher, Cat. No. 10828028) was added. To ensure successful thaw and expansion, NPCs were frozen at a density of $1x10^6$ cells per cryovial. Cryovials were stored at -80°C for 48hrs, then transferred to liquid nitrogen for long-term storage.

To expand NPCs, neural rosette clusters were resuspended in NIM. Cells were grown on pre-coated PLO-laminin plates, at relatively high densities. NIM was changed daily for 3-5 days (~80% confluent). To expand NPCs, cells were rinsed with DMEM/F12 and trypsinized (0.05%) for 3 minutes. Trypsin was then inactivated with DMEM/12 supplemented with 20% FBS and cells were collected. After centrifugation at 750 rpm for 3 minutes, the cell pellet was resuspended in NIM, and gently pipetted up-and-down to dissociate large cell clumps. Cells were passaged onto pre-coated PLO-laminin plates and fed daily until reaching 85-95% confluency. It is critical to culture NPCs at a high density for the successful maintenance of a stable and expandable population of progenitors; thus, when passaging NPCs, cells should be split at a 1:3 dilution. NPCs were characterized using immunocytochemistry (ICC) and qPCR to confirm the expression of markers including PAX6, SOX2, and NESTIN, in addition to the absence of SOX10. This approach produces a high percentage of PAX6 positive (96 ± 4%) and NESTIN positive (93 ± 3%) cells.

Immunocytochemistry

Culture medium was aspirated, and cells were washed and fixed with 4% paraformaldehyde (Sigma). Cells were washed and permeabilized with permeabilization buffer (0.1% Triton X-100 in PBS). Cells were then blocked

in 0.1% bovine serum albumin (BSA; Sigma) and treated with primary and secondary antibodies diluted in 0.1% BSA. Immunostained cells were then imaged (Nikon Eclipse 80i fluorescent microscope). The following antibodies were used: SOX2 (Life Technologies A24759), SSEA4 (Life Technologies A24866), Tra1-60 (Life Technologies A24868), OCT4 (Life Technologies A24867), NANOG (Life Technologies N4413), PAX6 (Abcam ab5790), NESTIN (Abcam, ab6142); DAPI (Life Technologies R37606); Alexa488 anti-rabbit (Life Technologies A32731); and Alexa594 anti-mouse (Life Technologies A24872).

Quantitative PCR

RNA was extracted from cell pellets with a RNeasy kit (Qiagen), following the manufacturer's protocol. Extracted RNA (10ug) was converted to cDNA by PCR using the High-Capacity cDNA Reverse Transcriptase kit (Life Technologies). Gene expression was measured in iPSCs using qPCR as previously described using Taqman (Life Technologies) probes (*SOX2* [Hs04260357_g1], *POU5F1* [Hs04260367_gH], *LIN28A* [Hs00702808_s1], *NANOG* [Hs04260366_g1], *B3GALT5* [Hs00707757_s1], *PODXL* [Hs01574644_m1], *SEV* [AI5IPH9]) (Karch et al., 2012). Capacity to spontaneously differentiate into the three germ layers was assessed using primers specific to cell-types found within the ectoderm, mesoderm, and endoderm (*ACTA2* [Hs00426835_g1], *AFP* [Hs00173490_m1], *DES* [Hs00157258_m1], *FN1* [Hs00277509_m1], *FOXA2* [Hs00232764_m1], *GFAP* [Hs00909233_m1], *TUBB3* [Hs00801390_s1]). Primers specific to *GAPDH* [Hs99999905_m1] used as a loading control.

Karyotyping

Chromosomal abnormalities were assessed by G-band karyotyping after clonal isolation of iPSC; after genome editing; and every 20 passages.

Supplemental References

Ban, H., Nishishita, N., Fusaki, N., Tabata, T., Saeki, K., Shikamura, M., Takada, N., Inoue, M., Hasegawa, M., Kawamata, S., *et al.* (2011). Efficient generation of transgene-free human induced pluripotent stem cells (iPSCs) by temperature-sensitive Sendai virus vectors. Proceedings of the National Academy of Sciences of the United States of America *108*, 14234-14239.

Budde, J., Martinez, R., Hsu, S., Wen, N., Chen, J., Coppola, G., Goate, A.M., Cruchaga, C., and Karch, C.M. (2017). Precision genome-editing with CRISPR/Cas9 in human induced pluripotent stem cells bioRxiv.

Karch, C.M., Jeng, A.T., Nowotny, P., Cady, J., Cruchaga, C., and Goate, A.M. (2012). Expression of novel Alzheimer's disease risk genes in control and Alzheimer's disease brains. PloS one *7*, e50976.

Murray, M.E., Cannon, A., Graff-Radford, N.R., Liesinger, A.M., Rutherford, N.J., Ross, O.A., Duara, R., Carrasquillo, M.M., Rademakers, R., and Dickson, D.W. (2014). Differential clinicopathologic and genetic features of late-onset amnestic dementias. Acta Neuropathol *128*, 411-421.

Perry, D.C., Brown, J.A., Possin, K.L., Datta, S., Trujillo, A., Radke, A., Karydas, A., Kornak, J., Sias, A.C., Rabinovici, G.D., *et al.* (2017). Clinicopathological correlations in behavioural variant frontotemporal dementia. Brain *140*, 3329-3345.

Sohn, P., Tracy, T., Huang, C., Yan, R., Camargo, C., Mok, S., Freilich, R., Roberson, E., Karch, C., Gestwicki, J., *et al.* (2019). Pathogenic Tau Impairs Axon Initial Segment Plasticity and Excitability Homeostasis. Neuron.

Takahashi, K., and Yamanaka, S. (2006). Induction of pluripotent stem cells from mouse embryonic and adult fibroblast cultures by defined factors. Cell *126*, 663-676.

Wang, C., Ward, M.E., Chen, R., Liu, K., Tracy, T.E., Chen, X., Xie, M., Sohn, P.D., Ludwig, C., Meyer-Franke, A., *et al.* (2017). Scalable Production of iPSC-Derived Human Neurons to Identify Tau-Lowering Compounds by High-Content Screening. Stem Cell Reports *9*, 1221-1233.